NTNU

Norwegian University of
Science and Technology

Calibration Technique for Quantitative Chloride Measurements with μ-XRF in Cementitious Materials

Rannei Ida Kaasa

Civil and Environmental Engineering
Submission date: June 2018
Supervisor: Klaartje De Weerdt, KT
Co-supervisor: Tobias Alexander Danner, KT

Norwegian University of Science and Technology
Department of Structural Engineering

Department of Structural Engineering
Faculty of Engineering
NTNU- Norwegian University of Science and Technology

ACCESSIBILITY

OPEN

MASTER THESIS 2018

SUBJECT AREA:	DATE:	NO. OF PAGES:
Concrete Technology	June 2018	77

TITLE:

Calibration Technique for Quantitative Chloride Measurements with μ-XRF in Cementitious Materials

Kalibreringsteknikk for kvantitative kloridmålinger med μ-XRF i sementholdige materialer

BY:

Rannei Kaasa

SUMMARY:

Corrosion due to ingress of chlorides is one of the major deterioration mechanisms of reinforced concrete structures exposed to seawater or de-icing salts. The chlorides are transported through the porous cement paste in the concrete. Corrosion will initiate when the chloride content in vicinity of the reinforcement reaches a critical limit. To determine the chloride content, a concrete core is profile ground to obtain concrete powder at different depth intervals. Subsequently, a wet chemical analysis e.g. potentiometric titration of the powder is performed. Wet chemical analysis is a precise, but time-consuming and labour-intensive method.

A less labour-intensive method recently introduced is micro X-Ray fluorescence (μ-XRF). With μ-XRF, elemental mappings e.g. chloride maps of split or sawn concrete surfaces can be determined. However, the signal of μ-XRF (counts per second=CPS) is not in a unit describing a concentration e.g. percentage of weight. As the chlorides are mainly present in the cement paste, a calibration curve relating the CPS of chlorine to a weight percentage of cement paste has to be established if μ-XRF is to be applied for determining the chloride content in cementitious materials.

In this study, cement paste samples with different water-to-cement ratio and known chloride contents were prepared. To study the effect of storage, paste samples were stored in isopropanol and on a desk. All samples were analysed by μ-XRF and a calibration curve was plotted based on the measured CPS of chlorine and the chloride content of the samples.

A technique for measuring the chloride content of mortar and concrete samples with μ-XRF was established. Based elemental maps from the μ-XRF and by use of software, the cement paste and aggregates were differentiated. The area percentage of aggregates and the CPS for the cement paste were obtained from the differentiation. The accuracy of the technique was then evaluated by comparing the chloride content determined by μ-XRF with the chloride content determined potentiometric titration. As the chloride content from titration was given by weight of concrete, a calculation model relating the CPS directly to the chloride content by weight of concrete was established. The basis of the calculation model was the calibration curve and the area percentage of aggregates.

The measurements resulted in a linear relation between the CPS and the chloride content of paste samples. In the range of 0.0 to 1.2% chlorides by weight of paste, the relation was found to be independent of the water-to-cement ratio. The relation can be used as a calibration curve to determine chloride contents of cement paste by μ-XRF. Furthermore, the detection limit of μ-XRF was found be lower than that of titration.

The results revealed that the parameters used for performing elemental mappings have an effect on the differentiation of the cement paste and aggregates. Which will consequently affect the determination of chloride content in the paste. For low chloride contents, the technique gave comparable results with the chloride content from titration of the mortar samples. However, for high chloride contents the results deviated. Except for one sample, comparable results with the titration were also obtained for the concrete samples, indicating that the technique can be used to determine chloride contents in cementitious materials. The technique had especially good accuracy for chloride contents near the critical chloride limit. However, the storage of the samples was found to have an effect of the measured CPS. These effects should be studied further to determine the proper storage of cementitious samples prior to μ-XRF measurements.

RESPONSIBLE TEACHER: Klaartje De Weerdt

SUPERVISOR(S): Klaartje De Weerdt, Tobias Danner, Mette Geiker

CARRIED OUT AT: NTNU Trondheim

Institutt for konstruksjonsteknikk
Fakultet for ingeniørvitenskap og teknologi
NTNU- Norges teknisk- naturvitenskapelige universitet

TILGJENGELIGHET

Åpen

MASTEROPPGAVE 2018

FAGOMRÅDE:	DATO:	ANTALL SIDER:
Betongteknologi	Juni 2018	77

TITTEL:

Kalibreringsteknikk for kvantitative kloridmålinger i sementholdige materialer

Calibration Technique for Quantitative Chloride Measurements in cementitious materials

UTFØRT AV:

Rannei Kaasa

SAMMENDRAG:

Kloridindusert armeringskorrosjon er en av de viktigste nedbrytningsmekanismene av armerte betongkonstruksjoner utsatt for sjøvann eller avisningssalter. Kloridene blir transportert via vann i den porøse sementpastaen i betong. Korrosjon som følge av kloridinntrenging vil initieres når kloridkonsentrasjonen i nærheten av armeringen når en viss terskelverdi. For å bestemme kloridkonsentrasjonen blir en betongkjerne frest til betongstøv i ulike dybdesjikt. Deretter gjennomføres en våtkjemisk analyse, som for eksempel potensiometrisk titrering, av betongstøvet. Våtkjemisk analyse er en presis, men tid- og arbeidskrevende metode.

En nylig introdusert og mindre arbeidskrevende metode er mikro røntgenfluorescens (μ-XRF). Med μ-XRF kan elementfordeling, som for eksempel kloridfordeling, av delte eller sagde betongoverflater bestemmes. Signalet fra μ-XRF er gitt i forekomster per sekund (counts per second=CPS) og er ikke en enhet som beskriver en konsentrasjon, som for eksempel vektprosent. Da kloridene hovedsakelig finnes i sementpastaen, må det opprettes en kalibreringskurve som relaterer CPS av klor til en konsentrasjon i prosent av sementpastavekt for å kunne anvende μ-XRF til å bestemme kloridinnholdet i sementholdige materialer.

I denne studien ble sementpastaprøver med forskjellige vann-til-sementforhold og kjent kloridinnhold støpt. Noen av prøvene ble lagret i isopropanol og andre på et skrivebord for å studere effekten av ulike typer lagring. Prøvene ble analysert ved μ-XRF og en kalibreringskurve ble fremstilt ved å plotte målt CPS av klor som funksjon av kloridinnholdet.

En metode for måling av kloridinnholdet i mørtel- og betongprøver ved μ-XRF ble etablert. Ved bruk av elementfordelinger fra μ-XRF og programvare ble sementpasta og aggregater differensiert. Basert på differensieringen ble CPS for sementpastaen og arealprosentandel av tilslag funnet. Nøyaktigheten av metoden ble deretter evaluert ved å sammenligne kloridinnholdet bestemt ved μ-XRF med kloridinnholdet bestemt ved potensiometrisk titrering. Ettersom kloridinnholdet fra titrering var gitt i prosent av betongvekt ble det etablert en beregningsmodell som relaterte CPS direkte til kloridinnholdet i vektprosent av betong. Grunnlaget for beregningsmodellen var kalibreringskurven og arealprosentandelen av tilslag.

Målingene resulterte i et lineært forhold mellom CPS og kloridinnholdet i pastaprøvene. I området fra 0,0 til 1,2% klorider av pastavekt var forholdet uavhengig av vann-til-sementforholdet. Forholdet kan brukes som en kalibreringskurve for å bestemme kloridinnholdet av sementpasta ved μ-XRF. Deteksjonsgrensen av klorider ble funnet til å være lavere for μ-XRF enn for titrering.

Resultatene viste at parameterne brukt for å bestemme elementfordelingene har en påvirkning på differensieringen av sementpasta og tilslag. Dette vil følgelig påvirke bestemmelsen av kloridinnholdet i pastaen. For lave kloridinnhold i mørtelprøvene ga teknikken sammenlignbare resultater med kloridinnholdet bestemt ved titrering. For høye kloridinnhold derimot ga teknikken avvik. Bortsett fra én prøve, ble sammenlignbare resultater med kloridinnholdet fra titrering av betongprøver også oppnådd hvilket indikerer at teknikken kan brukes for å bestemme kloridinnhold i sementholdige materialer. Teknikken hadde særlig god nøyaktighet for kloridinnhold nær terskelverdien. Lagringen av prøvene ble funnet til å ha en påvirkning på målt CPS. Disse påvirkningene bør undersøkes ytterligere for å kunne avgjøre hvilken type lagring som er best før måling ved μ-XRF.

FAGLÆRER: Klaartje De Weerdt

VEILEDER(E): Klaartje De Werdt, Tobas Danner, Mette Geiker

UTFØRT VED: NTNU Trondheim

Preface

This master thesis concludes the author's master's degree program of Civil and Environmental Engineering at NTNU, with specialization in concrete technology. The paper was written in 20 weeks during the spring semester 2018 and is a continuation of the associated specialization project *μ-XRF Calibration with respect to Chlorides in Cement Paste*, written during the fall semester 2017. The author is a civil engineering student and has only basic knowledge of radiation physics.

The main supervisor has been Associate Professor Klaartje De Weerdt, NTNU, and the co-supervisors have been Scientist Tobias Danner, NTNU and Professor Mette Geiker, NTNU.

The practical work associated to this master thesis has been carried out at the concrete laboratories of the Department of Structural Engineering at NTNU.

Acknowledgements

I would like to sincerely thank my main supervisor Klaartje De Werdt and co-supervisor Tobias Danner for all of the time they spent guiding me through this thesis. I had little experience with concrete technology before I started and a lot to learn. Their engagement in my work has motivated me and opened my eyes to how interesting the field of concrete technology is. I would also like to thank Tone Anita Østnor for her teaching and contagiously positive spirit, motivating me to learn more. Huge thanks are also owed to the staff at the NTNU concrete laboratories for guidance with my experiments, especially Steinar Seehus.

Abstract

Corrosion due to ingress of chlorides is one of the major deterioration mechanisms of reinforced concrete structures exposed to seawater or de-icing salts. The chlorides are transported through the porous cement paste in the concrete. Corrosion will initiate when the chloride content in vicinity of the reinforcement reaches a critical limit. To determine the chloride content, a concrete core is profile ground to obtain concrete powder at different depth intervals. Subsequently, a wet chemical analysis e.g. potentiometric titration of the powder is performed. Wet chemical analysis is a precise, but time-consuming and labour-intensive method.

A less labour-intensive method recently introduced is micro X-Ray fluorescence (μ-XRF). With μ-XRF, elemental mappings e.g. chloride maps of split or sawn concrete surfaces can be determined. However, the signal of μ-XRF (counts per second=CPS) is not in a unit describing a concentration e.g. percentage of weight. As the chlorides are mainly present in the cement paste, a calibration curve relating the CPS of chlorine to a weight percentage of cement paste has to be established if μ-XRF is to be applied for determining the chloride content in cementitious materials.

In this study, cement paste samples with different water-to-cement ratio and known chloride contents were prepared. To study the effect of storage, paste samples were stored in isopropanol and on a desk. All samples were analysed by μ-XRF and a calibration curve was plotted based on the measured CPS of chlorine and the chloride content of the samples.

A technique for measuring the chloride content of mortar and concrete samples with μ-XRF was established. Based elemental maps from the μ-XRF and by use of software, the cement paste and aggregates were differentiated. The area percentage of aggregates and the CPS for the cement paste were obtained from the differentiation. The accuracy of the technique was then evaluated by comparing the chloride content determined by μ-XRF with the chloride content determined potentiometric titration. As the chloride content from titration was given by weight of concrete, a calculation model relating the CPS directly to the chloride content by weight of concrete was established. The basis of the calculation model was the calibration curve and the area percentage of aggregates.

The measurements resulted in a linear relation between the CPS and the chloride content of paste samples. In the range of 0.0 to 1.2% chlorides by weight of paste, the relation was found to be independent of the water-to-cement ratio. The relation can be used as a calibration curve to determine chloride contents of cement paste by μ-XRF. Furthermore, the detection limit of μ-XRF was found be lower than that of titration.

The results revealed that the parameters used for performing elemental mappings have an effect on the differentiation of the cement paste and aggregates. Which will consequently affect the determination of chloride content in the paste. For low chloride contents, the technique gave comparable results with the chloride content from titration of the mortar samples. However, for high chloride contents the results deviated. Except for one sample, comparable results with the titration were also obtained for the concrete samples, indicating that the technique can be used to determine chloride contents in cementitious materials. The technique had especially good accuracy for chloride contents near the critical chloride limit. However, the storage of the samples was found to have an effect of the measured CPS. These effects should be studied further to determine the proper storage of cementitious samples prior to μ-XRF measurements.

Sammendrag

Kloridindusert armeringskorrosjon er en av de viktigste nedbrytningsmekanismene av armerte betongkonstruksjoner utsatt for sjøvann eller avisningssalter. Kloridene blir transportert via vann i den porøse sementpastaen i betong. Korrosjon som følge av kloridinntrenging vil initieres når kloridkonsentrasjonen i nærheten av armeringen når en viss terskelverdi. For å bestemme kloridkonsentrasjonen blir en betongkjerne frest til betongstøv i ulike dybdesjikt. Deretter gjennomføres en våtkjemisk analyse, som for eksempel potensiometrisk titrering, av betongstøvet. Våtkjemisk analyse er en presis, men tid- og arbeidskrevende metode.

En nylig introdusert og mindre arbeidskrevende metode er mikro røntgenfluorescens (μ-XRF). Med μ-XRF kan elementfordeling, som for eksempel kloridfordeling, av delte eller sagde betongoverflater bestemmes. Signalet fra μ-XRF er gitt i forekomster per sekund (counts per second=CPS) og er ikke en enhet som beskriver en konsentrasjon, som for eksempel vektprosent. Da kloridene hovedsakelig finnes i sementpastaen, må det opprettes en kalibreringskurve som relaterer CPS av klor til en konsentrasjon i prosent av sementpastavekt for å kunne anvende μ-XRF til å bestemme kloridinnholdet i sementholdige materialer.

I denne studien ble sementpastaprøver med forskjellige vann-til-sementforhold og kjent kloridinnhold støpt. Noen av prøvene ble lagret i isopropanol og andre på et skrivebord for å studere effekten av ulike typer lagring. Prøvene ble analysert ved μ-XRF og en kalibreringskurve ble fremstilt ved å plotte målt CPS av klor som funksjon av kloridinnholdet.

En metode for måling av kloridinnholdet i mørtel- og betongprøver ved μ-XRF ble etablert. Ved bruk av elementfordelinger fra μ-XRF og programvare ble sementpasta og aggregater differensiert. Basert på differensieringen ble CPS for sementpastaen og arealprosentandel av tilslag funnet. Nøyaktigheten av metoden ble deretter evaluert ved å sammenligne kloridinnholdet bestemt ved μ-XRF med kloridinnholdet bestemt ved potensiometrisk titrering. Ettersom kloridinnholdet fra titrering var gitt i prosent av betongvekt ble det etablert en beregningsmodell som relaterte CPS direkte til kloridinnholdet i vektprosent av betong. Grunnlaget for beregningsmodellen var kalibreringskurven og arealprosentandelen av tilslag.

Målingene resulterte i et lineært forhold mellom CPS og kloridinnholdet i pastaprøvene. I området fra 0,0 til 1,2% klorider av pastavekt var forholdet uavhengig av vann-til-sementforholdet. Forholdet kan brukes som en kalibreringskurve for å bestemme kloridinnholdet av sementpasta ved μ-XRF. Deteksjonsgrensen av klorider ble funnet til å være lavere for μ-XRF enn for titrering.

Resultatene viste at parameterne brukt for å bestemme elementfordelingene har en påvirkning på differensieringen av sementpasta og tilslag. Dette vil følgelig påvirke bestemmelsen av kloridinnholdet i pastaen. For lave kloridinnhold i mørtelprøvene ga teknikken sammenlignbare resultater med kloridinnholdet bestemt ved titrering. For høye kloridinnhold derimot ga teknikken avvik. Bortsett fra én prøve, ble sammenlignbare resultater med kloridinnholdet fra titrering av betongprøver også oppnådd hvilket indikerer at teknikken kan brukes for å bestemme kloridinnhold i sementholdige materialer. Teknikken hadde særlig god nøyaktighet for kloridinnhold nær terskelverdien. Lagringen av prøvene ble funnet til å ha en påvirkning på målt CPS. Disse påvirkningene bør undersøkes ytterligere for å kunne avgjøre hvilken type lagring som er best før måling ved μ-XRF.

Table of content

Abbreviations and list of symbols

Cement paste	–	Cement + Water + Added chlorides
Mortar	–	Cement + Sand + Water + Added chlorides
CPS	–	Counts per second
Dry cement	–	Hydrated cement paste dried at 950 °C
DTG	–	Derivative thermogravimetry
SDD-EDS	–	Silicon drift detector - energy dispersive spectroscopy
TGA	–	Thermogravimetric analysis
w/c-ratio	–	The mass ratio of water content to cement content
µ-XRF	–	Micro X-Ray fluorescence
wt-%	–	Weight percent
bwoc	–	By weight of cement

m	–	Mass [g]
M	–	Molar mass [g/mol]
w_T	–	Weight at a given temperature T in degrees Celsius [g]
C	–	Concentration [mol/l]
V	–	Volume [l]
ρ	–	Density [kg/m^3]
$\%Cl_{solution}$	–	Weight percentage of chlorides in a solution
$\%Cl_{bwoc}$	–	Percentage of chlorides by weight of cement
%NaCl	–	Weight percent of sodium chloride in the sodium chloride solution
$\%Cl_{paste\ 105°C}$	–	Percentage of chlorides determined by titration by weight of cement paste dried at 105 °C
%moisture	–	Moisture content by weight of cement paste at 105 °C
$\%Cl_{conc}$	–	Percentage of chloride by weight of concrete
$\%Cl_{conc\ µ\text{-}XRF}$	–	Percentage of chlorides by weight of concrete calculated with the calculation model
$\%Cl_{paste\ µ\text{-}XRF}$	–	Percentage of chlorides by weight of cement paste calculated with the equation obtained from the calibration curve
$\%H_2O$	–	Percentage of water content determined by thermogravimetric analysis
$\%Cl_{cem\ 950°C}$	–	Percentage of chlorides by weight of cement paste dried at 950 °C in a thermogravimetric device
$\%Cl_{conc\ 105°C}$	–	Percentage of chlorides determined by titration by weight of concrete dried at 105 °C
$\%Cl_{mort\ 105°C}$	–	Percentage of chlorides determined by titration by weight of mortar dried at 105 °C
$\%Agg_{µ\text{-}XRF}$	–	Area percentage of aggregates determined by µ-XRF
$\%Agg_{recipe}$	–	Volume percentage of aggregates calculated from concrete recipe

1 Introduction

1.1 Motivation

Corrosion of the steel reinforcement is one of the major deterioration mechanisms for reinforced concrete structures and leads to a reduction of the cross section of the reinforcing steel. As a result, the capacity of the structure will decrease [1]. The ingress of chlorides originates most often from exposure to seawater or de-icing salts. The chlorides may ingress through the porous cement paste in the concrete. The pores of the paste will contain a certain amount of water, called the pore solution. Chlorides may be transported into the pore solution by capillary suction, by diffusion or both.

Since the aggregates in the concrete are not as porous as the paste, the chlorides will mainly be present in the cement paste. Corrosion will be initiated when the chloride concentration in the vicinity of the reinforcement exceeds the critical chloride content threshold [2]. Since the critical chloride content for corrosion initiation is affected by a number of parameters, it is difficult to determine a general value [3]. In Europe and North America, 0.4% chloride by weight of cement is defined as the critical chloride content [4]. By weight of concrete, the critical chloride threshold can be considered to be 0.07% [5].

Considering the consequences of corrosion of the reinforcing steel on the structural capacity, there is a need for methods of measuring the chloride concentration and penetration depth in concrete. A traditional and well-established method of determining the chloride content in concrete cores is wet chemical analysis. For this method, a concrete core is extracted and profile ground to obtain concrete powder at different depth intervals. The powder is dissolved in acid and the resulting solution is filtrated and titrated to determine the chloride content [6]. This traditional method is precise, but time consuming, labour-intensive and therefore expensive. A novel recently introduced method is micro X-ray fluorescence (µ-XRF). With µ-XRF one can determine elemental maps e.g. chloride maps on split or sawn concrete surfaces [7]. This method is less labour-intensive compared to the traditional profile grinding method. In addition, one can determine the 2D spatial distribution of chlorides in the sample with the µ-XRF-method and thereby investigate phenomena where the chloride ingress fronts are complicated e.g. ingress along cracks and presence of distance holders for the reinforcement [8]. Whereas with the traditional profile grinding method one only obtains a 1D chloride profile (paste and aggregates) and an average chloride content for each section.

1.2 Research questions

The chlorine in the 2D spatial distributions from the µ-XRF is given in counts per second (CPS) while the critical threshold of chlorine is given by weight of cement or by weight of concrete. In order to relate the CPS of the µ-XRF measurements to a concentration by weight of cement or concrete, a calibration curve has to be established. This thesis aims to answer the following questions:

- Can cement paste samples with a known chloride content be mixed to establish a calibration curve relating the counts per second (CPS) obtained with the µ-XRF to the chloride concentration in the paste samples?
- Concrete is an inhomogeneous material containing cement paste and aggregates. Since the chlorides are mainly present in the cement paste, how can the cement paste be differentiated from the aggregates in the measurements?
- Can the calibration curve be used for determining the chloride concentration in the cement paste of concrete samples?
- Will the type of storage of cementitious samples affect the µ-XRF measurements?

1.3 Limitations

The scope of this study does not include a detailed insight into the radiation physics of µ-XRF measurements due to time restraints.

2 Theoretical background

2.1 Proportioning with regards to chloride content

As calibration samples, cement pastes with known chloride contents were prepared. The chlorides (Cl) can be added in the cement paste by mixing the dry cement with water and a solution containing chlorides. This could for example be sodium chloride (NaCl) dissolved in water. The weight percentage of chlorides in the solution is defined as

$$\%Cl_{solution} = \frac{m_{NaCl}\,[g]}{m_w[g] + m_{NaCl}[g]} \cdot \frac{M_{Cl}\,\left[\frac{g}{mol}\right]}{M_{NaCl}\,\left[\frac{g}{mol}\right]} \tag{1}$$

With m_{NaCl} the mass of NaCl salt, m_w the mass of water, M_{Cl} the molar mass of Cl (35.43 g/mol) and M_{NaCl} the molar mass of NaCl (58.44 g/mol).

The needed mass of solution to achieve the desired chloride content by weight of cement ($\%Cl_{bwoc}$) is given as

$$m_{solution} = \frac{\%Cl_{bwoc} \cdot m_{cement}\,[g]}{\%Cl_{solution}} \tag{2}$$

With m_{cement} the mass of cement.

The total mass of water, $m_{w,tot}$, in the cement mix is determined from the desired water-to-cement ratio (w/c-ratio) and the mass of cement. Since the NaCl solution contains water, the sum of the mass of water in the NaCl solution and the mass of pure water must be equal to the desired total mass of water. We define the mass of pure water to be added as

$$m_{w,added} = m_{w,tot} - \frac{100 - \%NaCl}{100} \cdot m_{solution} \tag{3}$$

where $\%NaCl$ is the wt-% of NaCl of the NaCl solution.

2.2 Micro X-ray fluorescence (µ-XRF)

The micro X-ray fluorescence (µ-XRF) relies on the same physical principle as the X-ray fluorescence (XRF) which is explained in the following paragraph. However, the spatial resolution, i.e. the spot size of the X-ray beam, is many orders of magnitude smaller than the regular XRF as a collimator focusses the beam. In addition, the µ-XRF is equipped with a sample table which can move the samples underneath the X-ray with a high precision, i.e. 5 µm. The combination of the collimator and the precise sample table permits the determination of elemental maps with a resolution down to approx. 20 µm.

XRF is a technique for analysing the elemental composition of a sample. To explain the principle, we use the simplified atom model from Bohr, the shell model (see Figure 1). When an X-ray beam hits an atom, it can eject an electron from one of the inner electron shells of the atom. With incompletely filled electron shells, the atom is in an unstable state. To correct this

instability, an electron from an outer electron shell will jump down to fill the vacancy of the ejected electron. For instance, if an electron is ejected from the K-shell, an electron from the L-shell, or the M-shell, will jump to the K-shell to fill the vacancy. The transition of an electron from an outer to an inner electron shell, results in the emission of energy in form of a photon. This is called fluorescence.

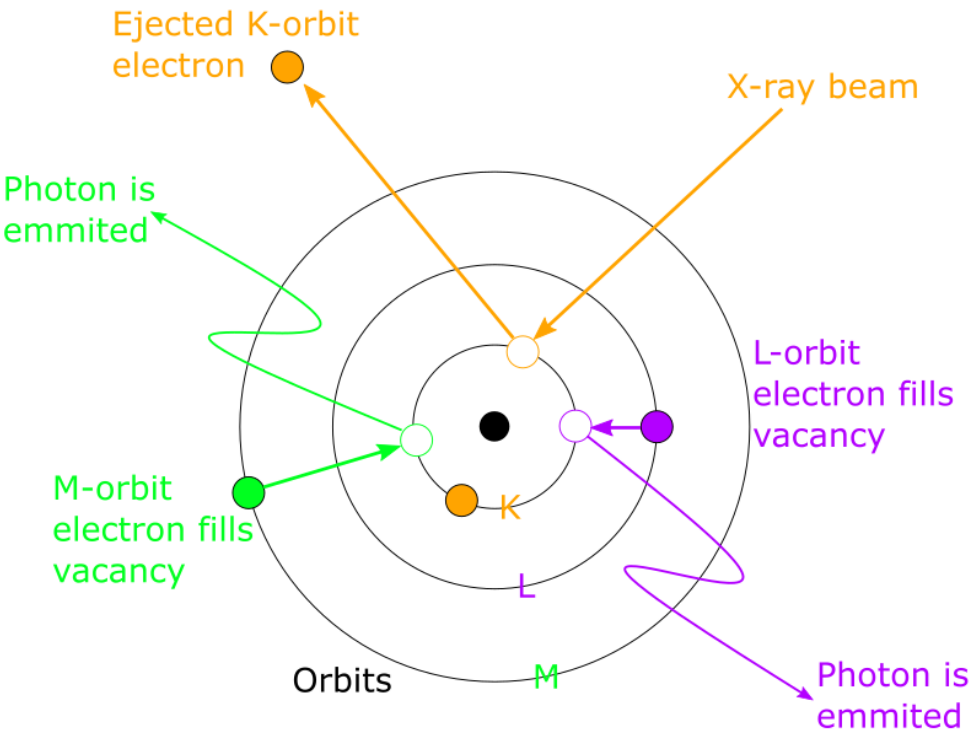

Figure 1: Visualization of the ejection and transition of electrons in an atom under the influence of radiation adopted from [9].

The emitted energy is equal to the energy the electron loses when it jumps to an electron shell closer to the nucleus of the atom. The energy binding an electron to its orbit increases as the distance from the orbit to the nucleus increases. Therefore, there is a loss in energy that is equivalent to the difference in the energy of the two electron shells. The lost energy is detected as a fluorescent signal. Since the energy level between the electron shells is unique for each element, one can determine the element based on the fluorescent signal registered.

The intensity of the fluorescent signal, given in counts per second (CPS), is correlated to the amount of the element. Using software, the CPS for each part of the energy spectrum is plotted. If the intensity for a certain energy is high, it is visualized as a peak. The software then associates the peaks in the energy spectrum to the characteristic energy level of the elements, and thereby determines intensities of the different elements in the analysed volume. As a result, we can get the peak intensities in CPS of the different elements present in the sample as shown in Figure 2.

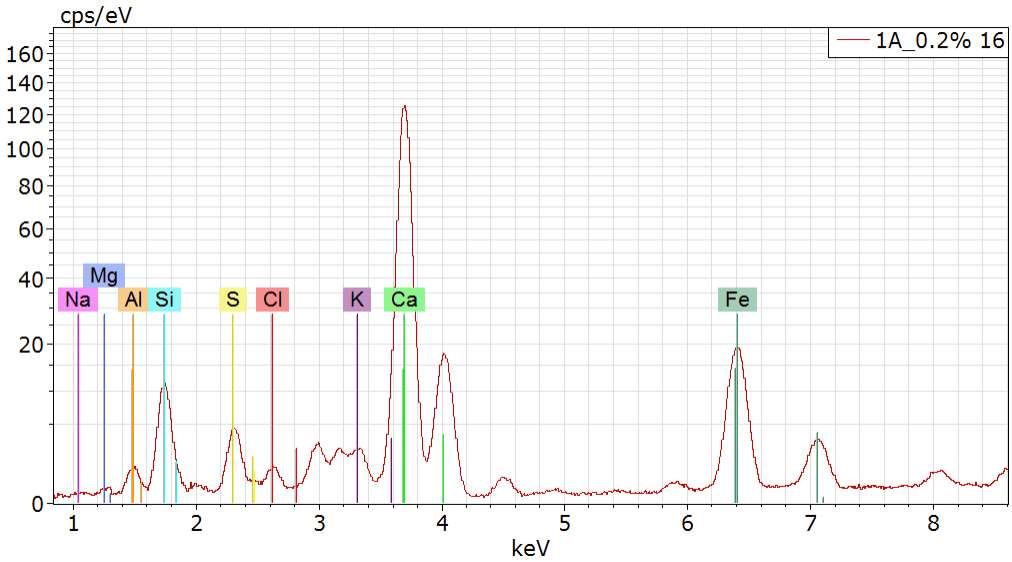

Figure 2: Peak positions at different energies (keV) and intensities (CPS) of elements in a cement paste sample.

One can compare the number of CPS obtained for an element in two similar samples and thereby obtain semi-quantitative results. For example, one can determine that sample A contains 20% more iron than sample B. These semi-quantitative results do not indicate the absolute quantity of an element in relation to a unit describing a concentration, e.g. parts per million or percentage of weight. A calibration is needed to correlate the measured peak intensities in CPS to a specific known concentration.

2.3 Thermogravimetric analysis (TGA)

Thermogravimetric analysis (TGA) is used to determine the amount of bound water and carbonates in reacted cement paste. In addition, it can also be used to identify and quantify hydration phases present in the hydrated cement paste. During a TG analysis, the weight changes are measured while heating the sample (e.g. from 30 to 950°C). The temperature, the heating rate and the atmosphere are controlled. Different hydration phases in a hydrated cement paste decompose at specific temperature intervals. When hydration phases decompose, they emit water or carbon dioxide and thereby cause a decrease of the mass of the sample. This decrease in mass at a given temperature interval can therefore be related to a type and quantity of a specific phase present in the sample.

2.4 Chloride content determination by titration

To determine the chloride content in a cement paste or a concrete sample, potentiometric titration can be performed. First, the cement paste is ground into powder and dissolved in hot acid. After dissolution of the cement paste the suspension is filtrated. The resulting filtrate is then used for titration. The potentiometric titration method consists of measuring the electro chemical potential with an Ag/AgCl electrode in a known amount of filtrate while adding the titrant fluid. When the titrant, in this case an $AgNO_3$ solution, is added to the sample, the Cl^- in the filtrate will react with Ag^+ and precipitate as AgCl. The potential measured by the electrode is related to the Cl concentration in the analysed solution. When all the Cl^- has precipitated as AgCl, a potential drop is observed. This corresponds to the equivalence point where in this case the amount of moles of added Ag^+ matched the amount of moles of Cl^-. Generally, the potential

is plotted as a function of the added volume of titrant and the derivative is calculated. The equivalence point will correspond to the maximum of the derivative.

Based on the measured volume of titrating fluid added at the equivalence point (V_{AgCl}), the concentration of the titrating fluid (C_{AgCl}) and the volume of the filtrate used ($V_{filtrate}$), we can calculate the Cl concentration in the filtrate ($C_{Cl,filtrate}$) using the following formula:

$$C_{AgCl}\left[\frac{mol}{l}\right] \cdot V_{AgCl}[l] = C_{Cl,filtrate}\left[\frac{mol}{l}\right] \cdot V_{filtrate}[l] \tag{4}$$

The amount of Cl in the cement paste as a mass percent of the cement paste at 105°C is determined with the following formula:

$$\%Cl_{paste\ 105°C} = \frac{C_{Cl,filtrate}\left[\frac{mol}{l}\right] \cdot 35.45\left[\frac{g}{mol}\right] \cdot V_{HNO_3}[ml] \cdot 0.001}{m_{cement\ paste}\ [g] \cdot (1 - 0.01 \cdot \%moisture)} \cdot 100 \tag{5}$$

With V_{HNO_3} the volume of acid used to dissolve the cement paste, $m_{cement\ paste}$ the mass of cement paste used and $\%moisture$ the percentage of moisture by weight of cement paste at 105°C.

2.5 Chloride content determination by µ-XRF

When determining the chloride content in concrete samples by potentiometric titration, ground powder of the concrete i.e. both cement paste and aggregates, is analysed. The chloride content is given by weight of concrete. However, chloride ions from the environment will only penetrate through the cement paste. The risk of corrosion is mainly dependent on the chloride content in the paste. Therefore, it is the chloride content in the cement paste is that is of interest.

The chloride intensity in the cement paste of concrete samples may be determined by µ-XRF. However, the signal of the µ-XRF (counts per second=CPS) is not given in a unit describing a concentration. Consequently, a calibration curve relating the signal of µ-XRF to a chloride concentration will have to be established. A calibration curve may be established by measuring the CPS of chlorine in cement paste samples with a known chloride content determined by potentiometric titration. By doing so, a relation between the CPS and the chloride content by weight of cement paste is obtained.

If the µ-XRF is to be applied for determining the chloride content of concrete samples, the CPS of only the cement paste must be obtained. This can be done by use of software which differentiates the aggregates from the cement paste. From the differentiation, the software can retrieve the CPS of chlorine in the cement paste only. The chloride content by weight of cement paste may then be calculated using the calibration curve.

The accuracy of the technique for determining chloride content in concrete samples can be tested by comparing the chloride content determined by the calibration curve with the chloride content determined by potentiometric titration. Determining the chloride content of concrete samples by potentiometric titration gives the chloride content by weight of concrete. However,

since cement paste samples were used in the calibration, the chloride content will be given by weight of cement paste and not by weight of concrete. In order to compare the chloride content determined by the calibration curve and by titration, a model relating the chloride content by weight of cement paste to weight of concrete must be established.

Such a model requires the amount or percentage of aggregates in the concrete to be known. The area percentage of aggregates ($\%Agg_{\mu\text{-XRF}}$) is obtainable with the µ-XRF software. The area percentage is based on the area of the aggregates compared to the whole area measured.

The following model assumes that the volume percentage of aggregates (V_{agg}/V_{conc}) is the same as the area percentage of aggregates. Furthermore, it is assumed that the density of aggregates (ρ_{agg}) and the density of cement paste (ρ_{cem}) are known and that chlorides are bound solely in the cement paste. The chloride content by weight of concrete can be expressed as

$$\%Cl_{conc} = \frac{m_{Cl}}{m_{conc}} = \frac{m_{Cl}}{m_{paste}} \cdot \frac{m_{paste}}{m_{conc}} = \frac{m_{Cl}\,[kg]}{m_{paste}\,[kg]} \cdot \frac{\rho_{paste}\,[kg/m^3] \cdot V_{paste}\,[m^3]}{\rho_{conc}\,[kg/m^3] \cdot V_{conc}\,[m^3]} \quad (6)$$

With m_{Cl} the mass of chlorides, m_{conc} the mass of concrete, m_{paste} the mass of cement paste, ρ_{paste} the density of cement paste, ρ_{conc} the density of concrete, V_{paste} the volume of cement paste and V_{conc} the volume of concrete. If the amount of chlorides in the cement paste, m_{Cl}/m_{paste}, is determined by a calibration curve with a linear relationship i.e. y = ax + b, the ratio can be expressed as:

$$\frac{m_{Cl}}{m_{paste}} = \%Cl_{paste\ \mu-XRF} = ax + b \quad (7)$$

By using the fact that the density of a material is equal to the mass divided by the volume, that the mass of concrete is the sum of the mass of aggregates and cement paste and that the mass of cement paste is the sum of the mass of water and cement, the chloride content by weight of concrete can be determined with the following equation:

$$\%Cl_{conc\ \mu-XRF} = \%Cl_{paste\ \mu-XRF} \cdot \frac{\rho_{paste} \cdot \left(1 - \%Agg_{\mu-XRF}\right)}{\rho_{agg} \cdot \%Agg_{\mu-XRF} + \rho_{paste} \cdot \left(1 - \%Agg_{\mu-XRF}\right)} \quad (8)$$

With $\%Agg_{\mu-XRF}[\%]$ the area percentage of aggregates and assumed equal to the volume percentage of aggregates and $\rho_{agg}[kg/m^3]$ the density of the aggregates. The density of cement paste, $\rho_{paste}[kg/m^3]$, is defined as:

$$\rho_{paste} = \frac{\rho_w[kg/m^3] \cdot \rho_{cem}[kg/m^3] \cdot \left(\frac{w[kg]}{c[kg]} + 1\right)}{\rho_{cem}[kg/m^3] \cdot \frac{w[kg]}{c[kg]} + \rho_w[kg/m^3]} \quad (9)$$

With $\frac{w}{c}$ water-to-cement-ratio i.e. the mass of water divided the mass of cement, ρ_w the density of water (1000 kg/m^3) and ρ_{cem} the density of cement (3150 kg/m^3). Refer to Appendix A.1 for further details regarding the derivation of equations 8 and 9.

3 Experimental program

3.1 Cement paste sample preparation

3.1.1 Materials

As chlorides only penetrate through the cement paste, the micro X-Ray fluorescence (μ-XRF) calibration was performed using cement paste samples with a known chloride content. In Norway, Anleggsement, a CEM I 52,5N according to EN197 [10], produced by Norcem AS is a Portland cement frequently used for structures exposed to chlorides from seawater or de-icing salts. Therefore, it is a relevant choice of cement type with regards to chloride ingress.

Another relevant choice of cement could be Anleggsement FA, a CEM II/A-V 42.5N according to EN197 [10], a cement containing 18% fly ash. Anleggsement FA is the most frequently used cement type in Norway. However, for capacity reasons, only the Norcem Anleggsement without fly ash was chosen in this study. Adding fly ash might increase the required curing time as fly ash continues to react considerably over a longer time (months) compared to ordinary Portland cement. The chemical and physical properties of the cement are presented in Appendix A.2. The analyses were performed by Norcem AS.

As previously mentioned, the European and North American norm define 0.4% Cl by the weight of cement as the critical chloride content [4]. Based on concrete recipes found in an article by De Weerdt et al. [11], a chloride content of 1% by weight of concrete was found to correspond to approx. 4.4% by weight of cement. Five cement paste samples were prepared with chloride contents ranging from very low (near critical chloride content) to relatively high chloride contents. The chosen chloride concentrations for the calibration samples were 0.0, 0.2, 0.4, 1.5, 3.0 and 4.0% by weight of cement (see Table 3.1). Sodium chloride (NaCl) solutions were used to add chlorides to the paste samples.

Initially, the maximum chloride content was set to 5% by weight of cement in order to include maximum concentrations observed in concrete profiles from real structures [11]. However, the consistency of cement pastes with 5% chloride content was clay-like, probably due to accelerated setting caused by a high NaCl content. Therefore, the maximum chloride content was reduced to 4% by weight of cement.

The cement powder may contain an amount of chlorides [12]. This amount of chlorides has to be specified as a maximum limit of chloride content by the producer. The batch of Anleggsement used in this study has a maximum limit of chloride content of 0.025% by weight of cement as specified by Norcem AS (see Appendix A.2). The samples with the sample names and corresponding intended chloride content are given in Table 3.1. The chloride contents in Table 3.1 do not take into account the maximum limit of chloride content in the cement powder.

Table 3.1: Intended chloride content in wt-% of cement in the samples, not accounting for the maximum limit of chloride content.

Intended chloride content [wt-% of cement]	**Samples with w/c = 0.4**	**Samples with w/c = 0.6**
0.0	PC 0.4-0.0	PC 0.6-0.0
0.2	PC 0.4-0.2	PC 0.6-0.2
0.4	PC 0.4-0.4	PC 0.6-0.4
1.5	PC 0.4-1.5	PC 0.6-1.5
3.0	PC 0.4-3.0	PC 0.6-3.0
4.0	PC 0.4-4.0	PC 0.6-4.0

Two solutions with different concentrations of NaCl (5 and 25 wt-%) were used to add chlorides to the paste samples. The NaCl solutions were made by pouring 50 and 250 g of NaCl in two 1000 ml volumetric flasks and filling them with distilled water. The NaCl was not dried prior to making the solutions. The NaCl used was of type 12314 with a purity grade of minimum 99.0%, produced by Alfa Aesar. Considering the varying density of NaCl dissolved in water, the concentrations were in fact 4.8 and 21.1 wt-% NaCl, respectively. Refer to Appendix A.3 for details regarding measured values and calculations.

The reason for using two different concentrations was to achieve the chosen w/c-ratio in all paste samples with varying chloride contents. Samples PC 0.4-1.5, PC 0.4-3.0, PC 0.4-4.0, PC 0.6-3.0 and PC 0.6-4.0 could not be mixed with 4.8 wt-% NaCl because the total mass of water, based on the w/c-ratio, would be exceeded.

3.1.2 Mix proportions, mixing and curing

From NS-EN 206:2013+NA2014, Table NA.12 [13] we can see that the durability classes M45, MF45, M40 and MF40 are allowed when considering exposure to chlorides (i.e. exposure classes XS1-XS3 and XD1-XD3 [13]). For these durability classes, the water-to-binder-ratio varies from 0.45 to 0.40 given the different cement types. Based on this, a w/c-ratio of 0.4 was used for one series of paste samples. To study the possible effect of porosity on the peak intensity measured with μ-XRF, a series of samples with w/c-ratio of 0.6 was prepared as well. The cement paste recipes used are given in Table 3.2.

Table 3.2: Cement paste recipe.

Sample	CEM I 52,5N [g]	4.8 wt-% NaCl solution [g]	21.1 wt-% NaCl solution [g]	Water [g]
PC 0.4-0.0	100.00	-	-	40.00
PC 0.4-0.2	100.00	6.59	-	33.61
PC 0.4-0.4	100.00	13.19	-	27.21
PC 0.4-1.5	100.00	-	9.89	31.61
PC 0.4-3.0	100.00	-	19.78	23.22
PC 0.4-4.0	100.00	-	26.38	17.63
PC 0.6-0.0	100.00	-	-	60.00
PC 0.6-0.2	100.00	6.59	-	53.61
PC 0.6-0.4	100.00	13.19	-	47.21
PC 0.6-1.5	100.00	49.45	-	12.05
PC 0.6-3.0	100.00	-	19.78	43.22
PC 0.6-4.0	100.00	-	26.37	37.63

All the quantities were measured with a PA413C model Ohaus Pioneer precision balance which has a readability of 0.001 grams. However, the precision of the third decimal was low so the results are rounded to two decimals. Subsequently, the materials were continuously mixed for one minute with a Braun MultiQuick 3 hand blender at speed 11 in a 350 mL Braun MQ 20 chopper accessory. To avoid false set, the paste rested for one minute before remixing for another minute. An accumulation of cement was observed underneath the blade of the hand blender. By the use of a spatula, this accumulation was remixed with the rest of the materials. After mixing, the cement paste was poured into four tubes with a diameter of 2 cm. The height of the samples varied from about 2 cm to 2.5 cm. The tubes were sealed with a lid and parafilm. Finally, the samples were stored in a sealed box at a constant temperature of 20ºC in a climate room before sawing. The samples with w/c-ratio of 0.4 were stored for 28 days, while the samples with w/c-ratio of 0.6 were stored for 15 weeks.

3.1.3 Sawing and storage

The sawing of the paste samples was performed using an IsoMet 1000 precision saw produced by Buehler. About 2 mm of the bottom of the samples was sawed off and discarded. Then the samples were sawn to obtain 5 mm discs. The remaining part of the samples i.e. the top of the sample was also discarded. The discs were submerged in isopropanol in plastic boxes, sealed with parafilm and stored in a desiccator over silica gel. The isopropanol was produced by Lab-Scan Analytical Sciences and had a purity of minimum 99.7%. Additionally, four discs were stored on the desk in the laboratory exposed to air.

Using a second tube of the same batch, about 2 mm of the bottom of the tube was sawn off and discarded. This time, a 10 mm disc was sawn off. The top was discarded. The 10 mm discs were crushed into powder in a porcelain mortar using a pestle. The powder was poured into a plastic bag with ziplock sealing and stored in a desiccator over silica gel. Later, the powder was used for thermogravimetric analysis (TGA) and determination of the chloride content by potentiometric titration.

3.2 Mortar sample preparation

3.2.1 Materials

In order to test the applicability of micro X-Ray fluorescence (µ-XRF) to examine the chloride content in cementitious samples with aggregates, mortar samples with known chloride content were also cast. In this way, potential matrix effect (e.g. absorption of X-Rays by inhomogeneous density) influencing the counts per second (CPS) output from µ-XRF measurements can be evaluated as well. The samples were made with Anleggsement, a CEM I 52,5N according to EN197 [10], produced by Norcem AS. The cement was from the same batch as the cement used in the cement paste samples. As aggregate, CEN-Standard Sand according to EN 196-1 [14] produced by Normensand GmbH was used.

To include concentrations most likely present in concrete samples from real structures, four mortar samples were made with intended chloride (Cl) concentrations of 0.0, 0.4, 1.5 and 4.0% by weight of cement. The chloride concentrations were chosen by the same reasoning as for the cement paste samples. The samples with sample names and corresponding intended chloride content are given in Table 3.3.

Table 3.3: Intended chloride content in wt-% of cement of the mortar samples, not accounting for the maximum limit of chloride content in the cement.

Intended chloride content [wt-% of cement]	**Sample**
0.0	M 0.5-0.0
0.4	M 0.5-0.4
1.5	M 0.5-1.5
4.0	M 0.5-4.0

As for the cement paste samples, a sodium chloride (NaCl) solution was used to add chlorides to the mortar samples. A 25 wt-% NaCl solution was prepared by mixing 250 g NaCl and 750 g distilled water in a 1000 ml flask. The sodium chloride used was from the same batch from Alfa Aesar used in the cement paste samples. The NaCl was not dried prior to making the solution.

3.2.2 Mix proportions, mixing and curing

The composition of the mortar samples was according to the Norwegian Standard NS-EN 196-1 [14] and is given in Table 3.4. The w/c-ratio was 0.5.

Table 3.4: Mortar recipe.

Sample	**CEM I 52,5N [g]**	**CEN Sand [g]**	**25 wt-% NaCl solution [g]**	**Water [g]**
M 0.5-0.0	450	1348	-	225.0
M 0.5-0.4	450	1349	11.9	216.1
M 0.5-1.5	450	1350	44.5	191.7
M 0.5-4.0	450	1350	118.7	135.9

The sand was weighed on a Mettler Toledo PM6000 with 0.1 g readability. To determine the exact amount of sand, the plastic bag of sand was weighed prior to mixing. Afterwards, the

weight of the empty plastic bag was subtracted. The water and NaCl solution were weighed on a Mettler Toledo PM2000 weight with 0.01 g readability. The cement was weighed on a Mettler Toledo SB32001 Delta Range weight with 0.1 g readability. Due to the low precision of the last decimal of the weights used, the results are rounded to one decimal for the weight of water and NaCl and to a whole number for the weight of cement and sand.

The mixing was performed according to the mixing procedure of mortar samples described in NS-EN 196-1 [14]. The materials were mixed using a Hobart N50 mixer with a "B" flat beater. First, cement and water were mixed for 30 seconds before steadily adding sand for 30 seconds on low speed. Next, the mixer was stopped for 30 seconds to scrape down any residue on the sides of the mixing bowl. The mix was left to rest for another 60 seconds. Finally, the mix was mixed for another 60 seconds on medium speed. The mortars were cast in moulds of 40x40x160 mm. The moulds were first filled halfway using a spatula and vibrated for a few seconds. Subsequently, the moulds were filled to the top and vibrated for a second time before removing excess mortar. During the first 24 hours the mortars were cured in the laboratory while the top of the moulds was lightly covered with plastic to avoid drying out before demoulding. After demoulding, the samples were packed in water tight foil and placed in a sealed box. The samples were then stored at a constant temperature of 20ºC in a climate room for 27 days before sawing.

3.2.3 Sawing

Bleeding when moulding cementitious material is a known phenomenon [15]. Free water in the mix will be pushed to the surface as the heavier particles such as aggregates and cement settle. Bleeding was observed for samples M 0.5-0.0 and M 0.05-4.0 and a lower chloride content than the recipe is expected. Due to this, the cast mortar prisms could have a higher concentration of chlorides at the surface and cause the samples to be inhomogeneous. Bleeding will also result in a higher w/c-ratio at the surface of the mould.

The wall effect is a phenomenon describing the packing of aggregates near a wall [16]. The spacing between the aggregates close to a wall is larger than the spacing deeper in the concrete. To avoid any wall effects, 10 mm was sawn off each surface of the mortar prisms with a water-cooled concrete saw using the minimal amount of water. Subsequently, the now 20x20x140 mm prisms were sawn in half using a saw without water cooling. An approx. 10 mm thick disc was sawn off one half and an approx. 20 mm thick disc was sawn off the other half as can be seen in Figure 3. The discs were wrapped in clingfilm and placed in separate ziplock bags. The ziplock bags were stored in a desiccator over silica gel. The 10 mm thick discs were used for μ-XRF measurements. The 20 mm thick discs were grounded into powder using a Retsch RS 200 mill. The chloride content of the powder was found by potentiometric titration.

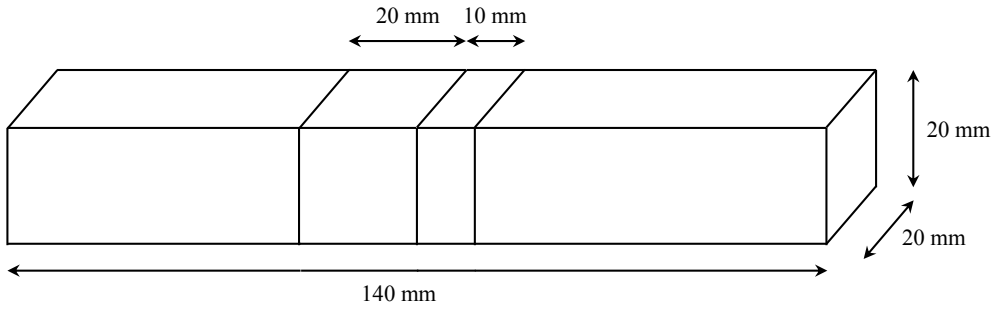

Figure 3: Schematic of the sawing of the mortar prisms.

3.3 Concrete samples

All investigated concrete cores were taken from field exposed structures with 100 mm diameter using a water-cooled concrete core drilling machine. Concrete core samples 2-B-2 and 2-T-2 were extracted from concrete columns exposed to natural seawater for 33 years [17]. They were produced by Norwegian Contractors in Hinnavågen by order of DNV GL, using the same procedures and routines as in normal offshore production. The concrete recipe and w/c-ratio of samples 2-B-2 and 2-T-2 are shown in Table 3.5.

Table 3.5: Concrete recipe for samples 2-B-2 and 2-T-2 [17].

Constituent	**Mass**
Cement	420 kg
Aggregates	1870 kg
Water	160 kg
w/c-ratio	0.38

Concrete core sample RSD was extracted from Hafrsfjord Bridge in September 2017. The foundation from which the core was extracted, was exposed to seawater in the tidal zone. The Hafrsfjord Bridge was built in 1967 and documentation of the concrete composition of sample RSD was not available. However, it is known that the concrete in the foundation is of B300 quality as defined in the Norwegian Standard NS 427 A [18] published in 1962, which was the standard at the time of the construction of the bridge. A B300 concrete is equivalent with a w/c-ratio of 0.6 [19]. Based on this, it is assumed in this study that sample RSD has a w/c-ratio of 0.6.

Concrete sample BAR was extracted from the atmospheric/wave zone of a 3000x300x150 mm concrete column submerged in sea water in Sandnessjøen for 25 years [20]. The setup of the experiment if shown in Figure 4. The concrete recipe of sample BAR is given in Table 3.6.

Figure 4: Setup of the experiment of which sample BAR was a part of [20].

Table 3.6: Concrete recipe for sample BAR [20].

Constituent	**Mass [kg/m^3]**
Binder*	388.5
Aggregates	1865
Water	160.5
Equivalent w/c-ratio**	0.4

*Cement and 4% silica fume by weight of cement
** Efficiency factor of 2 for silica fume

3.4 Chloride content determination by titration

In order to determine the exact amount of chlorides in the cast cement paste and mortar samples and the investigated concrete cores, a potentiometric titration was performed. The samples were grounded into a fine powder and dried at 105°C. 50 ml of 80°C nitric acid (HNO_3) with a concentration ratio of 1:10 was added to the dried powder. The suspension was then stirred and left to stand for one hour. Using syringes equipped with microfilters, about 10 mL of the suspension was filtered and transferred to plastic tubes. Finally, a potentiometric titration was conducted using a Titrando 905 titrator produced by Metrohm. 0.01 M silver nitrate ($AgNO_3$) was used as titrant. The procedure was performed on all cementitious samples.

The concrete cores were cut longitudinally into two halves to enable µ-XRF analysis on one half. The other half of the core was profile ground and the concrete powder at different depth intervals was analysed by titration. The depth intervals were up to 100 mm for sample 2-B-2, up to 60 mm for sample RSD and up to 50 mm for samples 2-T-2 and BAR. In the case of the cement paste samples, the entire titration process was performed on two parallels of each sample, meaning 12 filtrates in total.

3.5 Thermogravimetric analysis (TGA)

Ground, not dried samples of hydrated cement pastes were analysed with thermogravimetry to determine the amount of water (both free and bound) in the samples. By doing so, the chloride content by weight of cement paste from titration could be related to a chloride content by weight of dry cement. The analysis was performed on samples PC 0.4-0.0, PC 0.4-0.4, PC 0.4-3.0, PC 0.6-0.0, PC 0.6-0.4 and PC 0.6-3.0 using a Mettler Toledo TGA/DSC3+ device. Approx. 200 mg of the powder was poured into 600 µL corundum crucibles. The samples were heated from 40 to 950 °C with a heating rate of 10 °C/min, while the weight loss was measured. The oven was purged with 50 mL/min of nitrogen during the measurements. The sample weight at approx. 950 °C was assumed to be the dry cement weight. The percentage of water (%H_2O) was determined by the difference in weight of the sample between approximately 40 and 950°C using the following equation.

$$\%H_2O = \frac{w_{40} - w_{950}}{w_{40}} \cdot 100 \qquad (10)$$

With w_{40} the weight at 40°C and w_{950} the weight at 950°C.

3.6 Micro X-Ray fluorescence analysis

3.6.1 Cement paste samples

Cut discs of hydrated cement paste that were submerged in isopropanol and stored in a desiccator, were analysed by µ-XRF. The samples were lightly dried prior to measurements. The instrument used was a M4 Tornado from Bruker with a silicon drift detector for energy dispersive analysis (SDD-EDS). The µ-XRF is equipped with a silver X-ray tube and polycapillary lense focusing the X-ray beam to a spot size of 20 µm. No elemental filter was used. The signal of the µ-XRF (counts per second = CPS) was retrieved for chlorine (Cl) for all measurements. The measurement parameters for the elemental mappings are given in Table 3.7.

Table 3.7: Measurement parameters for analysis with µ-XRF.

Parameter	**Condition**
Chamber pressure	Vacuum, 20 mbar
Number of detectors	2
Tube current	600 µA
Accelerating voltage	50 kV
Dead time	< 20%
Filter	No filter

Elemental maps of the cement paste discs were taken with two activated detectors at a current of 600 µA and a voltage of 50 kV. The chamber pressure was 20 mbar at all times. All elemental mappings of the paste samples were taken with a speed of 1 ms per pixel and 35 µm distance between each measurement point. According to Bruker [9] a deadtime below 50% is recommended. The deadtime in these performed measurements was less than 20%. Subsequently, the object-function in the M4 Tornado Software was used to mark concentric areas of each sample in the mapping and the spectrums of the areas was retrieved. Refer to Figure 5 for illustration of the objects marked. The spectrum of the area is based on a summation and normalisation of the intensities of each of the pixel included in the area. The object-function was used twice to check the precision of the CPS. The CPS was used as input for the calibration curve and to examine the effect of different storage of the paste samples.

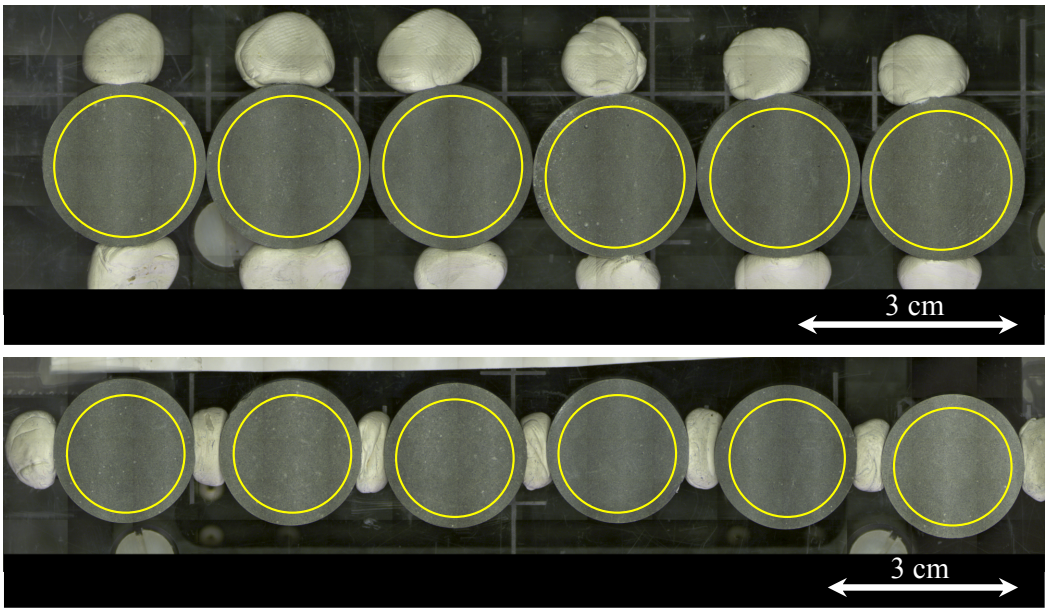

Figure 5: The areas marked by use of the object function are illustrated by the yellow circles. The samples with w/c-ratio of 0.4 are shown in the top image while the samples with w/c-ratio of 0.6 are shown in the bottom image.

Chlorine mappings are presented as false colour plots. These plots are purely qualitative and show a percentage of the differential range measured (CPS). The smallest value in the map is defined as "0" and the largest as "100". The measured range is defined by colours. Red colours indicate high values and blue colours indicate low values. All mappings are normalized individually. See Figure 6 and Figure 7 for the order of the samples in the elemental maps.

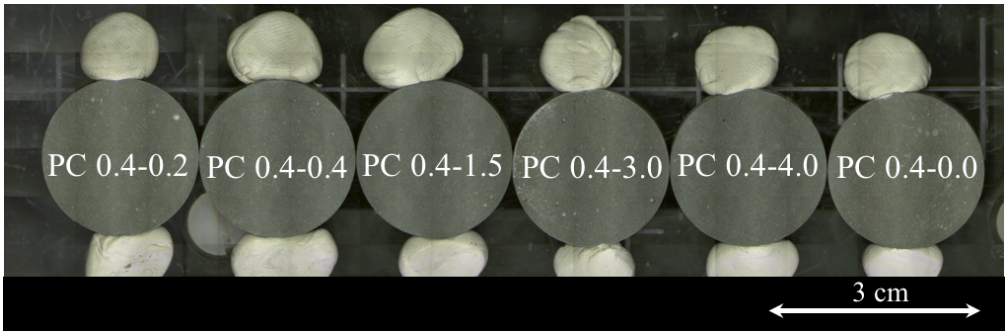

Figure 6: Setup for samples with w/c-ratio of 0.4 for elemental mappings.

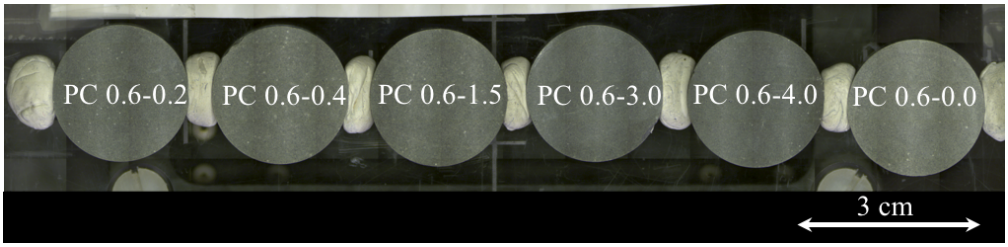

Figure 7: Setup for samples with w/c-ratio of 0.6 for elemental mappings.

3.6.2 Mortar samples

Cut discs of the cast mortar prisms with known chloride contents were also analysed in the M4 Tornado. An individual elemental mapping was performed for each mortar disc. The parameters were the same as for the elemental mapping of the cement paste discs (see Table 3.6), except that the elemental mappings of the mortar discs were taken with a step width of 10 µm and a collection time of 5 ms per pixel. The step width of the mapping initially set to 35 µm, but as the mapping became pixelated the step width was decreased to 10 µm. The dimensions of the mapping were 10x11 mm.

The M4 Tornado software allows for differentiation of areas of similar composition into several phases based on the elements chosen for the elemental mapping. By use of this feature, two phases were differentiated in each disc: the phase representing the cement paste and the phase representing the aggregates. Refer to Figure 8 for illustration of a phase differentiation. The background for the creation of the phases is the chemical information of each pixel included in the elemental mapping. The area percentage of each phase compared to the area of the whole mapping is calculated and a spectrum with intensities for different energies of the pixels included in the phase is created. As each phase contains several pixels, the individual intensities of each pixels are summed up and normalized for the total collection time of all the included pixels. The software also allows for combining two or more phases into one phase. The phases which appeared to represent the paste were combined and the same was done for the phases which appeared to represent the aggregates. The combination of phases was based on the subjective opinion of the author.

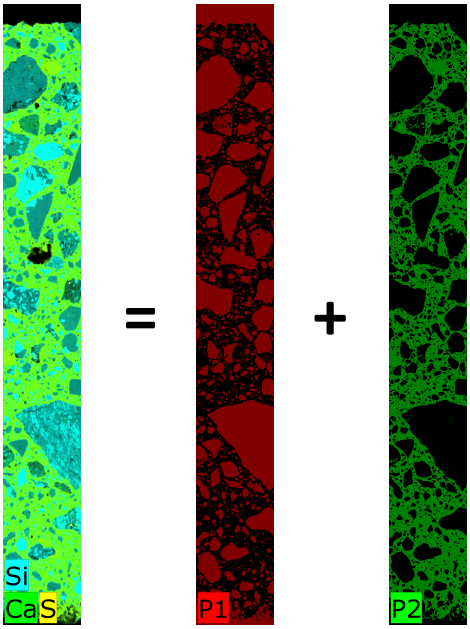

Figure 8: Phase differentiation of a concrete sample into an aggregate phase (red) and a cement paste phase (green) based on a sulphur-calcium-silica-elemental mapping (left).

Two differentiations of the sections in the mortar samples were performed, one based on a sulphur-calcium-silica-elemental map (S-Ca-Si-map) and one based on a calcium-silica-elemental map (Ca-Si-map). This was done to examine the possible effect the choice of elements has on the differentiation. For both differentiations, the area percentage of the aggregate phase and the spectrum of the cement paste phase were retrieved. The CPS of chlorine was obtained from the spectrum.

The CPS of chlorine was used to calculate the chloride concentration according to the calibration curve established by the µ-XRF measurements of the cement paste samples. The area percentage of aggregates was used as input in the calculation model relating the chloride concentration in wt-% of cement paste to wt-% of concrete (see equation 8).

3.6.3 Concrete samples

Elemental mappings of the sawn concrete cores were performed in layers equivalent to the depth intervals of the profile grounding used for potentiometric titration. The mappings were taken with a 5 ms per pixel collection time and a 35 µm step width. As for the mortar samples, the aggregates and cement paste were separated in an aggregate phase and a cement paste phase. For sample 2-T-2, different elements and combinations of elements were tested as the basis of the differentiation. The elemental maps tested were a sulphur-map (S-map), a sulphur-calcium-map (S-Ca-map) and a sulphur-calcium-silica-map (S-Ca-Si-map). Finally, the S-Ca-Si-map was chosen as the basis as it provided a visually better differentiation.

The spectrum for the cement paste phase was retrieved and the measured CPS for chlorine was noted. The CPS was used to calculate the chloride concentration by weight of cement paste according to the calibration curve established by the µ-XRF measurements of the cement paste sample. The area percentage of aggregates was also retrieved and used as input in the calculation model relating the chloride concentration in wt-% of concrete and wt-% of cement paste (see Equation 8).

In addition, elemental mappings of the entire surface of the concrete samples were performed. The software of the M4 Tornado cannot perform a mapping that takes longer than 2 hours to finish due to limitations of the hardware and software. Therefore, the collection times and step widths of the mappings of the entire surface of the concrete cores are different from those of the mapping of the layers. The collection times and step widths used in the mappings of the entire concrete cores are as given in Table 3.8.

Table 3.8: Collection time and step width of elemental maps of entire surface of concrete samples.

Sample	**Step width [μm]**	**Collection time [ms/pixel]**
2-T-2	40	1
2-B-2	40	1
BAR	45	1
RSD	50	1

4 Results

4.1 Thermogravimetric results

The thermogravimetric curves (TG) and their derivatives (DTG) for samples PC 0.4-0.0, PC 0.4-0.4 and PC 0.4-3.0 are shown in Figure 9. The same curves for samples PC 0.6-0.0, PC 0.6-0.4 and PC 0.6-3.0 are shown in Figure 10.

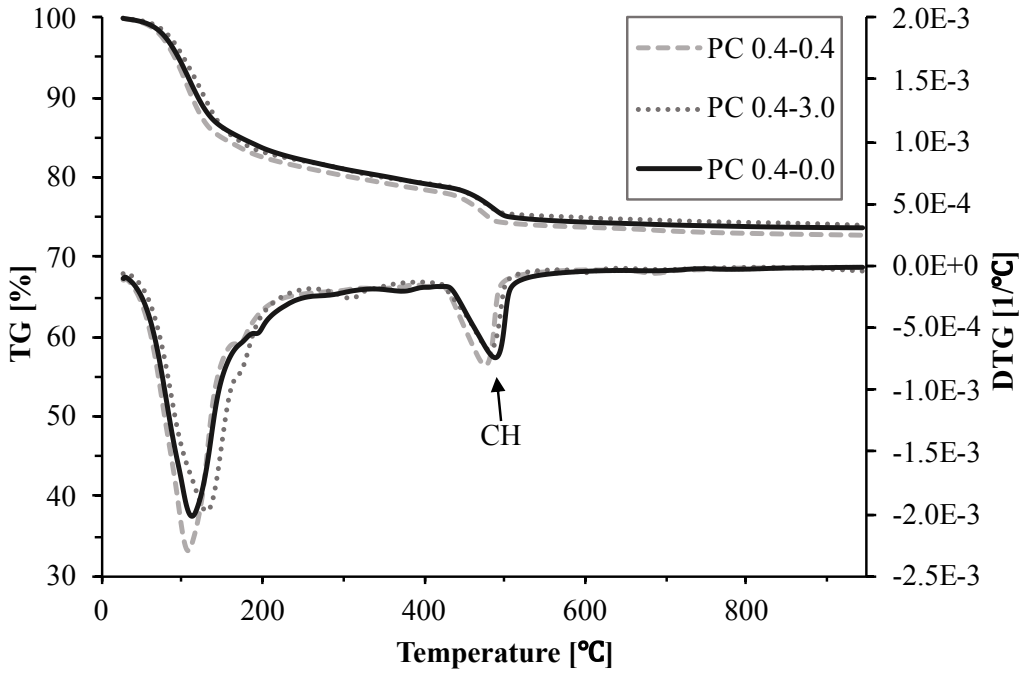

Figure 9: Thermogravimetric (TG) results (upper curves) and derivative thermogravimetric (DTG) results (lower curves) for samples PC 0.4-0.0, PC 0.4-0.4 and PC 0.4-3.0.

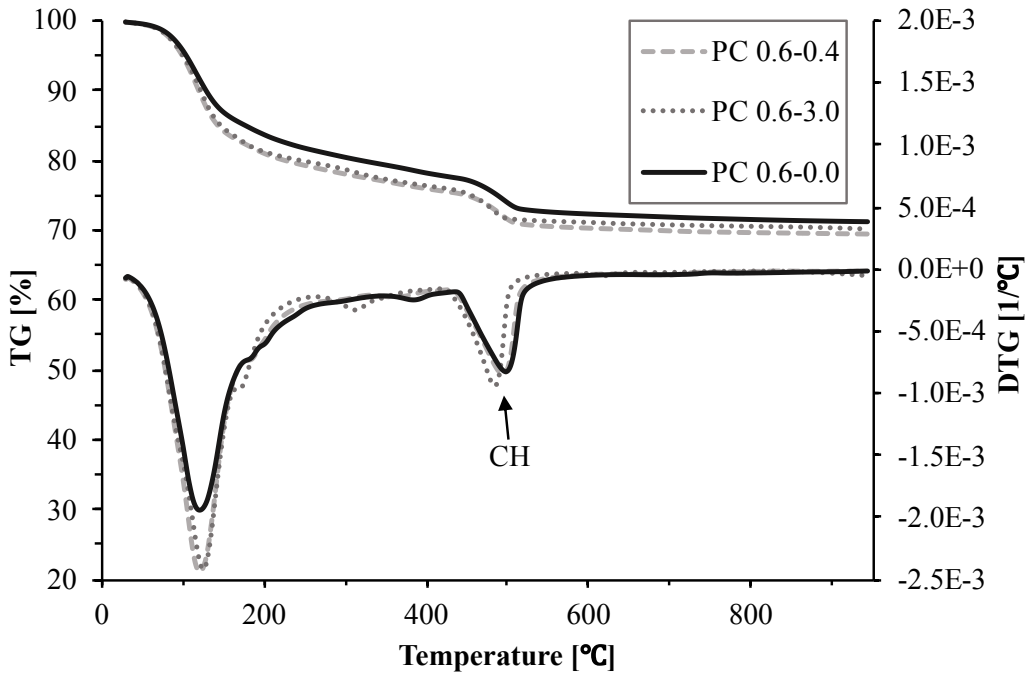

Figure 10: Thermogravimetric (TG) results (upper curves) and derivative thermogravimetric (DTG) results (lower curves) for samples for samples PC 0.6-0.0, PC 0.6-0.4 and PC 0.6-3.0.

The TG curves show that the samples have a mass loss of approx. 5% due to the decomposition of calcium hydroxide (CH). In addition, there are no signs of carbonation since the DTG curves show no peaks between 600 and 950°C.

The total amount of water in the samples with a w/c-ratio of 0.4 and 0.6 was approx. 26% and 30%, respectively. The total amount of water is both free and bound water since the samples weren't dried prior to analysis. The percentage of total mass loss, i.e. the water content, in the each of the analysed samples between approx. 40 and 950 °C is given in Table 4.1.

Table 4.1: Total mass loss from 40 to 950 °C determined by thermogravimetric analysis.

Sample	**Total mass loss [%]**
PC 0.4-0.0	26.27
PC 0.4-0.4	26.98
PC 0.4-3.0	25.99
Average	*26.41*
PC 0.6-0.0	28.76
PC 0.6-0.4	30.38
PC 0.6-3.0	29.50
Average	*29.55*

The samples with a w/c-ratio of 0.6 contained on average a higher total amount of water than the samples with a w/c-ratio of 0.4, as seen by the difference of approx. 3.5% between the averages. This is not surprising as cement paste with a w/c-ratio of 0.4 will not even in theory reach full hydration without water from an external source [21]. The samples with a w/c-ratio of 0.6 will have a higher degree of hydration since more water is available and therefore bind more water than the samples with a w/c-ratio of 0.4.

When looking at the DTG curves in the range from 100 to 450°C in Figure 11, peaks in the region from 150 to 200°C and from 300 to 350°C are observed. Peaks in a DTG curve of a cementitious material in these temperature regions are associated with the presence of AFm phases. The AFm phase called Friedel's salt is a chloride binding phase and is usually recognized by peaks in the region of 300 to 350°C [22]. Samples PC 0.4-3.0 and PC 0.6-3.0 contain the most Friedel's salt as can be seen by the larger peaks and have therefore bound more chlorides than the other samples. The DTG curves of samples PC 0.4-0.4 and PC 0.6-0.4 on the other hand, are hardly distinguishable from the reference samples.

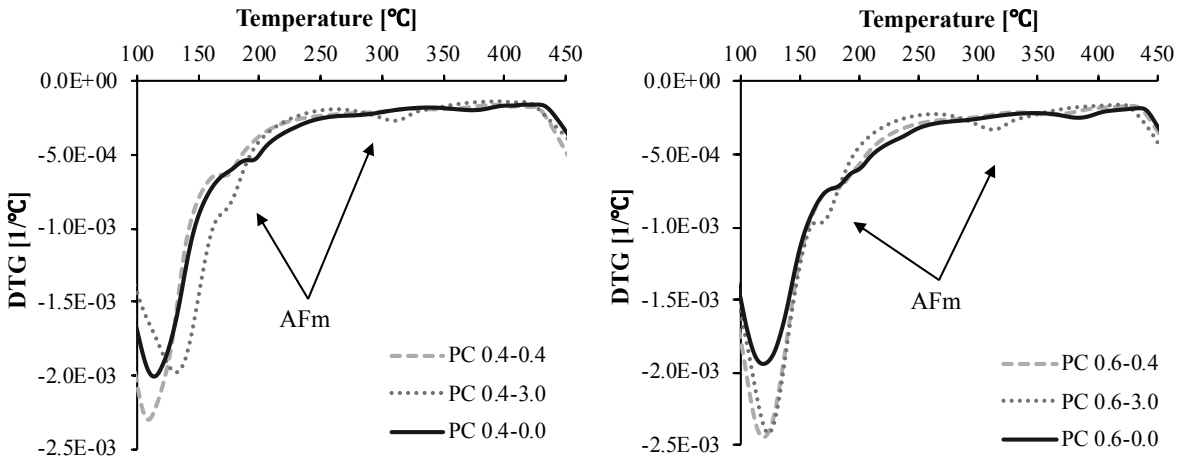

Figure 11: Derivative thermogravimetric (DTG) results in the range from 100 to 450 °C.

4.2 Chloride content determined by potentiometric titration

4.2.1 Cement paste samples

The chloride content in the paste samples determined by the potentiometric titration was averaged for the two test parallels performed on each sample in both samples series. The raw data from the titration is given in Appendix A.4. The chloride content of titration is given by weight of cement paste at 105°C ($\%Cl_{paste\ 105°C}$). The results of the titration were corrected for the average percentage of water content determined by the TGA, and thus expressing the chloride content by weight of dry cement at 950°C using the following equation:

$$\%Cl_{cem\ 950°C} = \frac{\%Cl_{paste\ 105°C}}{1 - \frac{\%H_2O}{100}} \tag{9}$$

With $\%Cl_{cem\ 950°C}$ the chloride content in wt-% of dry cement at 950°C, $\%Cl_{paste\ 105°C}$ the chloride content in wt-% of cement paste at 105°C determined by titration and $\%H_2O$ the average percent of water determined by TGA.

Table 4.2 shows the average chloride content by weight cement paste and by weight of dry cement including the relative uncertainty of the chloride content by weight of dry cement. These relative uncertainties were calculated by error propagation of the uncertainties in the titration and the thermogravimetric analysis assuming uncorrelated and random errors. See Appendix A.5 for details of the error propagation calculations.

Table 4.2: Average chloride content of dried cement paste at 105°C determined by titration, chloride content of dry cement at 950°C corrected for water content and its relative uncertainty.

Sample	Average $\%Cl_{paste\ 105°C}$ [wt-% of cement paste]	$\%Cl_{cem\ 950°C}$ [wt-% of dry cement]	Relative uncertainty $\%Cl_{cem\ 950°C}$ [%]
PC 0.4-0.0	invalid	-	-
PC 0.4-0.2	0.250	0.295	8
PC 0.4-0.4	0.395	0.458	8
PC 0.4-1.5	1.160	1.347	4
PC 0.4-3.0	1.827	2.135	4
PC 0.4-4.0	2.947	3.424	4
PC 0.6-0.0	0.009	0.013	8
PC 0.6-0.2	0.197	0.279	8
PC 0.6-0.4	0.290	0.412	8
PC 0.6-1.5	0.917	1.301	4
PC 0.6-3.0	1.503	2.134	4
PC 0.6-4.0	2.039	2.895	4

For the sample PC 0.4-0.0, the volume of filtrate used in the titration was 5 ml and resulted in an invalid result. The potential of the analyte dropped very fast after a very small amount of the titrating fluid was added due to the low chloride concentration. This resulted in an unprecise determination of the equivalence point. Therefore, the chloride content could not be determined precisely. In the titration of sample PC 0.6-0.0, the volume of filtrate was increased to 10 ml. By using a larger volume of filtrate, the equivalence point could be precisely determined, resulting in a valid value for the chloride concentration.

The relative uncertainties of $\%Cl_{cem\ 950°C}$ vary (4% and 8%) because different pipettes (1 ml and 5ml) with different uncertainties were used to measure the volume of filtrate used in the titration. The relative uncertainty of the chloride content of dry cement in sample PC 0.4-0.0 cannot be calculated since the measurement was invalid.

Figure 12 shows the chloride content by weight of dry cement determined by titration ($\%Cl_{cem\ 950°C}$) and the intended chloride content by weight of cement based on the added chlorides in the recipe. The uncertainties of $\%Cl_{cem\ 950°C}$ for each sample presented in Table 4.2 are represented by black error bars in the diagram.

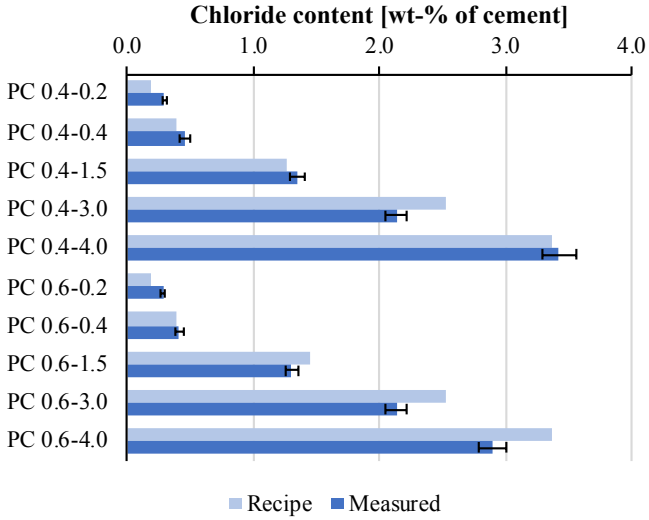

Figure 12: Comparison of the chloride content by weight of cement based on the added chloride in the recipe with the measured chloride content by titration by weight of dry cement at 950 °C. The uncertainties of the measured chloride content are represented by black error bars.

Samples PC 0.4-3.0, PC 0.6-3.0 and PC 0.6-4.0 have relatively large differences in the chloride content determined by titration and intended chloride content based on the added chlorides in the recipe. For all of these samples, the intended chloride content is higher than the chloride content measured by titration. The maximum difference in chloride content of 0.47% by weight of cement is observed in sample PC 0.6-4.0.

However, when plotting the intended chloride contents based on the recipe versus the chloride content measured by titration, the reliability index (R^2) of the trend line is 0.98, see Figure 13. A reliability index near 1.0 indicates a close to linear relation. All of the samples, except PC 0.4-0.0 which had an invalid titration result, are included in the plot.

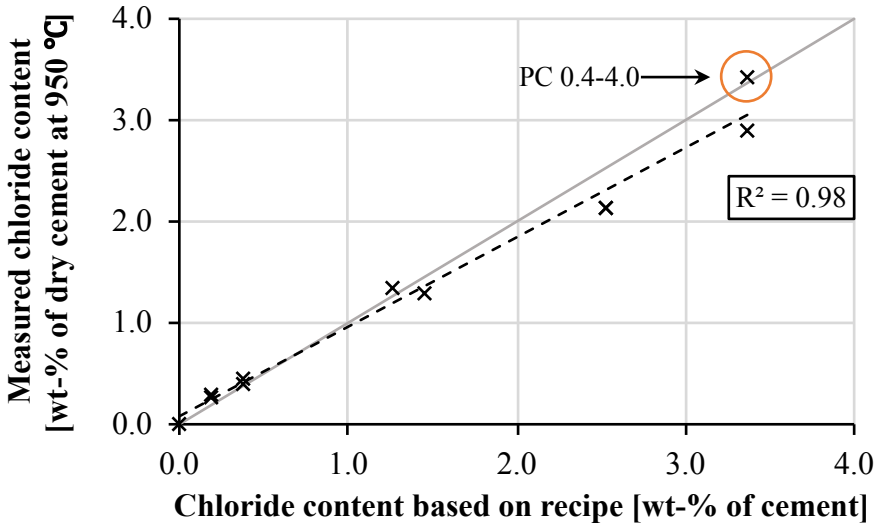

Figure 13: Chloride content by weight of cement based on the added chlorides in the paste recipes versus the chloride content dry cement (dried at 950 °C) determined by titration. Values for all cement paste samples of both sample series are included, except for sample PC 0.4-0.0 due to an invalid titration result. The grey line represents a 1:1-ratio.

As some of the samples had very similar chloride contents, the points in the plot may overlap. The trend line lies slightly below the grey line representing a 1:1-ratio. Considering the reliability index (R^2) of 0.98, the overall differences in chloride content of the samples are not significant. The samples with a chloride concentration above 2.0 wt-% of cement except for sample PC 0.4-4.0 are the samples which deviates the most from the 1:1-ratio.

4.2.2 Mortar samples

The chloride contents of the ground powder of the mortar samples were determined by titration. The chloride content in wt-% of mortar dried at 105°C including its relative uncertainty is given in Table 4.3. These relative uncertainties are calculated with error propagation of the uncertainties in the titration assuming uncorrelated and random errors. Refer to Appendix A.5 for details of the error propagation calculations.

Table 4.3: Chloride content by weight of mortar dried at 105°C ($\%Cl_{mort\ 105°C}$) and its relative uncertainty.

Sample	**$\%Cl_{mort\ 105°C}$ [wt-% of mortar]**	**Relative uncertainty $\%Cl_{mort\ 105°C}$ [%]**
M-0.5-0.0	invalid	-
M-0.5-0.4	0.099	6
M-0.5-1.5	0.334	3
M-0.5-4.0	0.868	3

The intended chloride content based on the added chloride content in the recipe is not included for the mortar samples. A thermogravimetric analysis to determine the chloride content by weight of dry mortar should be performed in order to determine the chloride content by weight of dry cement and thereby evaluate the mixing procedure of the mortar samples.

The volume of filtrate used in the titration of sample M 0.5-0.0 was 10 ml in an attempt to avoid an invalid result. Despite this, the chloride content in the sample was too low for the equivalence point to be precisely determined. Therefore, the chloride content in sample M 0.5-0.0 is set as invalid. The relative uncertainties of $\%Cl_{mort\ 105°C}$ vary (3% and 6%) since the volumes of filtrate were measured with different pipettes (1 ml and 5ml) with different uncertainties.

4.2.3 Concrete samples

The powders from the profile ground halves of concrete cores 2-T-2, 2-B-2, BAR and RSD, were analysed with potentiometric titration. The chloride content by weight of concrete at 105°C of all examined layers of the concrete samples is shown in Figure 14. Refer to Appendix A.6 for exact values of the chloride contents.

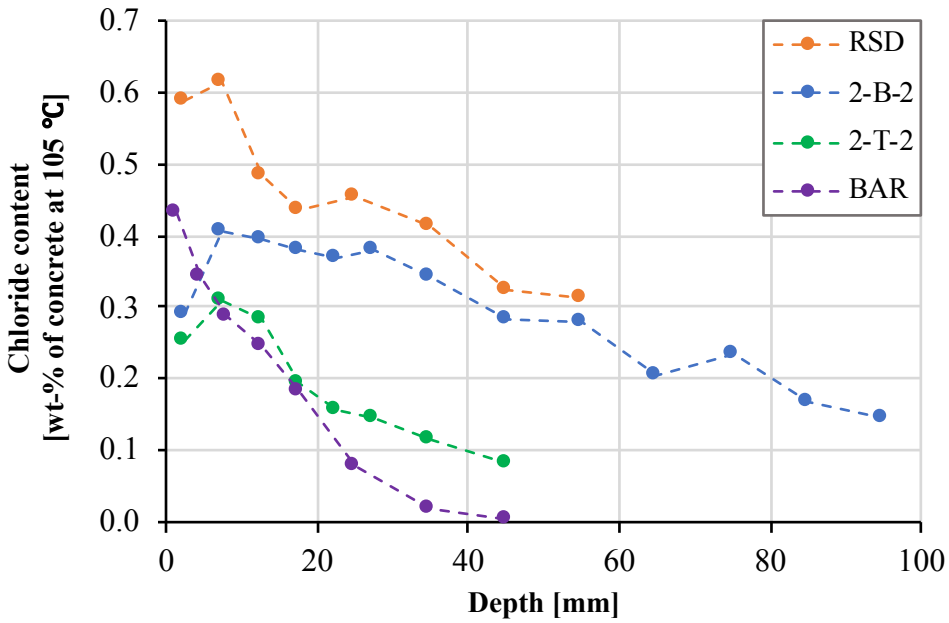

Figure 14: Chloride profiles by weight of concrete at 105 °C determined by titration of samples 2-T-2, 2-B-2, BAR and RSD. The chloride content of each layer is plotted at the depth of the middle of the layer.

The sample BAR is the only sample with chloride contents below the critical threshold (0.07 wt-% of concrete).

4.3 Micro X-ray Fluorescence measurements

4.3.1 Cement paste samples

The false colour plot of the chlorine mapping of the whole set of cement paste samples is shown in Figure 15.

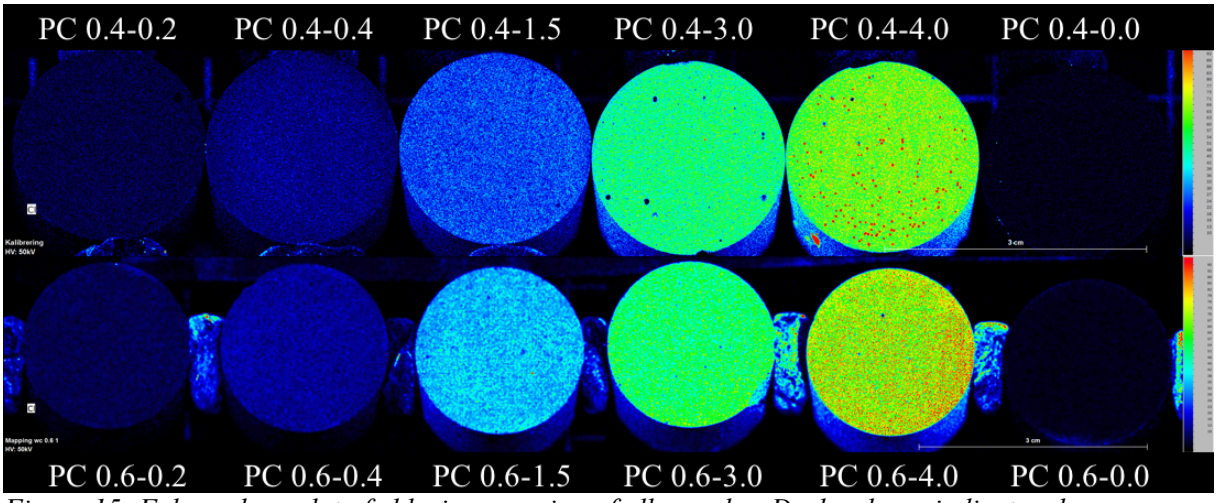

Figure 15: False colour plot of chlorine mapping of all samples. Dark colours indicate a low normalized value of CPS and red colours indicate a high normalized value of CPS. The plots are normalized individually. The diameter of the discs is 2 cm.

The reference samples to the far right are almost black indicating a very low chloride content compared to the other samples. Except for the reference samples, we can clearly see that the

CPS increases from the left to the right for both sample series. Sample PC 0.4-4.0 has a spotty appearance indicating locally increased chloride contents indicating that the sample has an inhomogeneous chloride content distribution. The inhomogeneity might be caused by the difficulty of mixing cement paste with a high chloride content due to accelerated setting. The homogeneity of sample PC 0.6-4.0 seems to be better, but it is still spotty. In addition, several air bubbles visible to the naked eye were observed in sample PC 0.4-3.0 which appear as dark spots in the false colour plot. The air bubbles might affect the μ-XRF measurements.

The CPS of chlorine for each sample were measured using the elemental mapping and the object-function (refer to Chapter 3.6.1). The CPS of were used as input for the calibration curve. Table 4.4 shows the measured CPS of chlorine for each sample.

Table 4.4: Counts per second (CPS) of chlorine using the mapping and the object-function.

Sample	**CPS**
PC 0.4-0.0	2.17
PC 0.4-0.2	5.25
PC 0.4-0.4	9.40
PC 0.4-1.5	20.7
PC 0.4-3.0	41.8
PC 0.4-4.0	56.4
PC 0.6-0.0	1.75
PC 0.6-0.2	4.27
PC 0.6-0.4	7.54
PC 0.6-1.5	20.4
PC 0.6-3.0	30.4
PC 0.6-4.0	41.5

The CPS of chlorine from Table 4.4 were plotted as a function of the chloride content of the paste samples determined by titration when dried at 105°C, see Figure 16. Sample PC 0.4-0.0 is not included as the chloride content was not precisely determined by titration. The trend line reliability (R^2) is 0.98 and 1.00 for sample series with w/c-ratio of 0.4 and 0.6, respectively, indicating that the linear trend lines are a good fit. The CPS can be considered as proportional to the chloride content determined by titration.

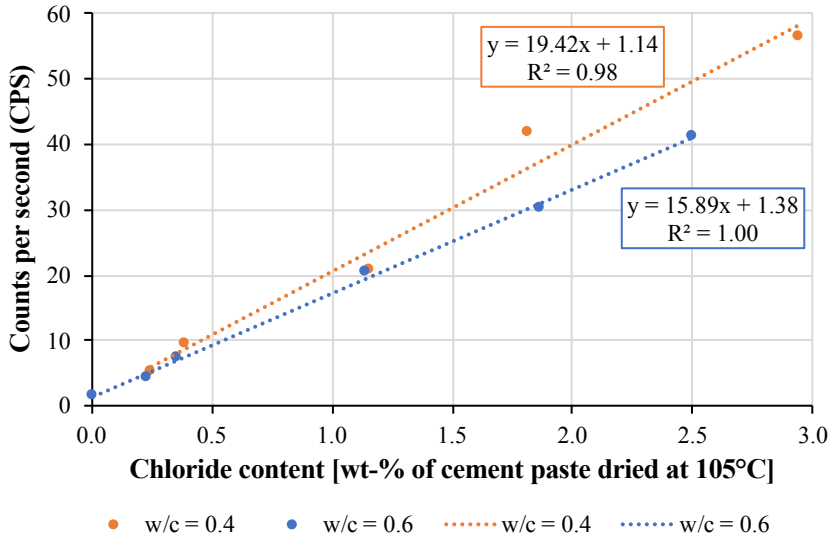

Figure 16: CPS of chlorine as a function of the chloride content of dried cement paste at 105 °C for cement paste samples with w/c = 0.4 (orange) and w/c = 0.6 (blue).

There is a slight difference in the slopes of the trend lines of the two sample series with different w/c-ratio. The y-intercept of the trend lines (1.14 and 1.38) are similar. For a CPS of 30, the trend line for w/c-ratio of 0.4 renders a chloride content of 1.49 wt-% of cement paste and the trend line for w/c-ratio of 0.6 renders a chloride content of 1.80 wt-% of cement paste. This results in a difference of 0.31% Cl by weight of cement paste between the two curves. A difference which will be even higher in wt-% of cement. When comparing with the critical chloride limit of 0.4% by weight of cement, the difference is significant.

4.3.2 Concrete and mortar samples

The phase differentiation (see Chapter 3.6.2) gives the area percentage of aggregates used in the calculation model relating the chloride concentration from wt-% of cement paste to wt-% of concrete (see Chapter 2.5). Using a sulphur-calcium-silica-elemental map (S-Ca-Si-map), each layer in all concrete samples was differentiated into aggregate and cement paste phases. The same process was performed on the entire surface of the concrete samples. In addition to the S-Ca-Si-map, the effect the elements chosen as the basis of the phase differentiation have on the calculation model was tested by differentiating sample 2-T-2 using a S-Ca-elemental map and a S-elemental map.

The area percentage of the aggregate phase ($\%Agg_{\mu\text{-XRF}}$) and the intensity of chlorine in counts per second (CPS) of the cement paste phase for samples 2-T-2 and 2-B-2, BAR and RSD are listed in Appendix A.7. The CPS of the cement paste phase were used to determine the chloride content by weight of cement paste according to the established calibration curve. The $\%Agg_{\mu\text{-XRF}}$ was utilized to relate the chloride content determined by the calibration curve in wt-% of cement paste to wt-% of concrete.

When the images of the phase differentiation of the layers in the samples were assembled into one image and compared to the phase differentiation of the entire surface, a variation of the area percentage of aggregates was observed. A differentiation based on a sulphur-calcium-silica-map (S-C-Si-map) taken in layers (top) and of the entire surface (bottom) of the concrete sample 2-B-2 is shown in Figure 17. The cement paste phase is the green area and the aggregate

phase is the red area. The differentiation of each layer is assembled into one image. The dimensions of both images are 100x100 mm.

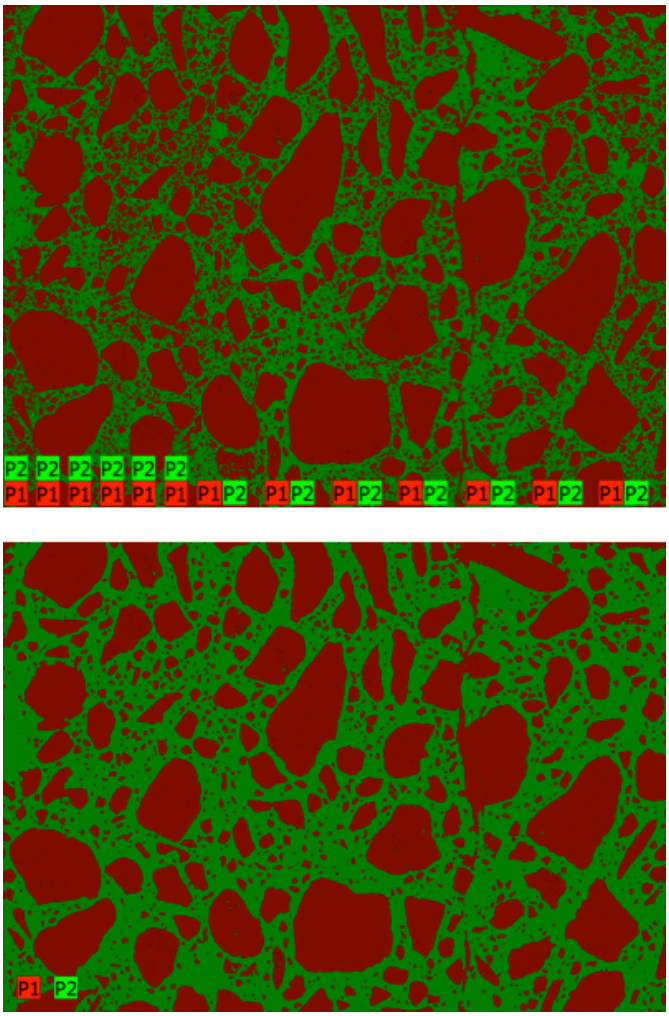

Figure 17: Differentiation based on a sulphur-calcium-silica-elemental map of sample 2-B-2 in aggregate phase (red) and cement paste phase (green) in layers (top) and of entire surface (bottom). The dimensions of the images are 100x100 mm.

Visually, the differentiation of the layers has a larger area percentage of aggregates than the differentiation of the entire surface. The only variables between the two mappings are the collection time and step width, i.e. 5 ms and 35 µm for the layers and 1 ms and 40 µm for the entire surface. The same observation was made for all concrete samples. Consequently, the collection time and step width seem to have an impact on the area percentage of aggregates and thus the determination of chloride content.

4.3.3 Mortar samples

The phase differentiation of the 10x11 mm section in the mortar samples was performed using a sulphur-calcium-silica-elemental map (S-Ca-Si-map) and a calcium-silica-elemental map (Ca-Si-map) as the basis of the differentiation. The aggregate and cement paste phases of sample M 0.5-1.5 based on a S-Ca-Si-map and a Ca-Si-map are shown in Figure 18.

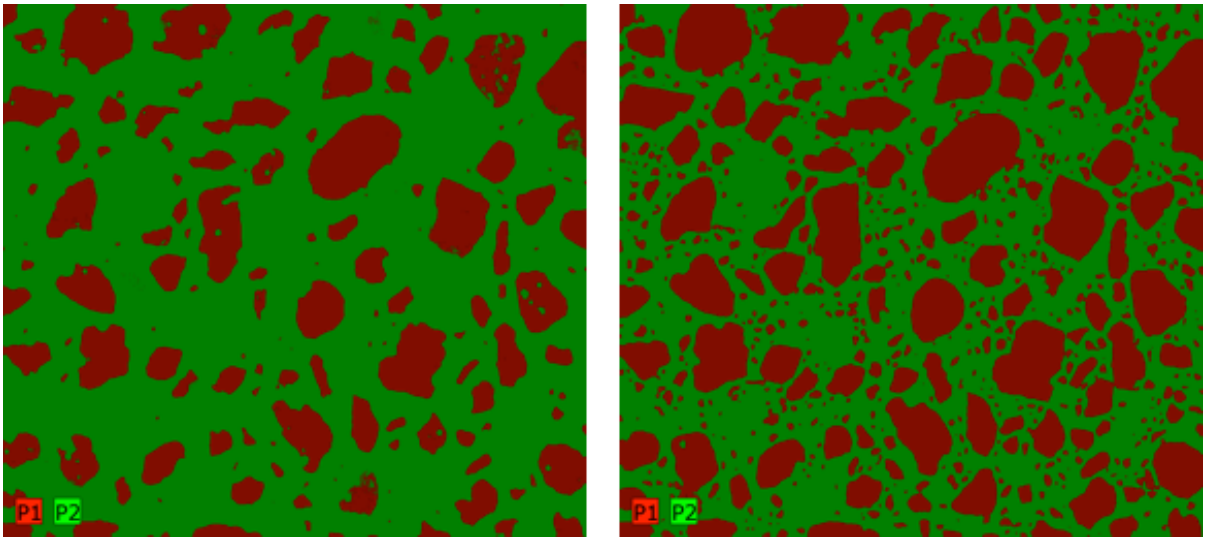

Figure 18: Phase differentiation of aggregates (red) and cement paste (green) of sample M 0.5-1.5 based on a sulphur-calcium-silica-elemental map (left) and based on a calcium-silica-elemental map (right). The dimensions of the images are 10x11 mm.

The area percentage of aggregates was retrieved for both elemental maps. The elemental maps gave very different area percentages of aggregates ($\%Agg_{\mu\text{-}XRF}$) i.e. 26.9 % from the S-Ca-Si-map and 43.9 % from the Ca-Si-map. This can even be observed visually from Figure 18. Consequently, the elements chosen as basis for the elemental mapping have an effect on the differentiation of phases of the mortar samples. The small area of the mapping resulted in a pixelated mapping when comparing with the mapping of the larger areas of the concrete samples. A good analogy is how an image can become pixelated when zooming in.

Furthermore, several air bubbles were observed in the elemental mapping of sample M 0.5-4.0 which could affect the measured counts per second (CPS). The air bubbles can be seen as black spots in the elemental mapping in Figure 19.

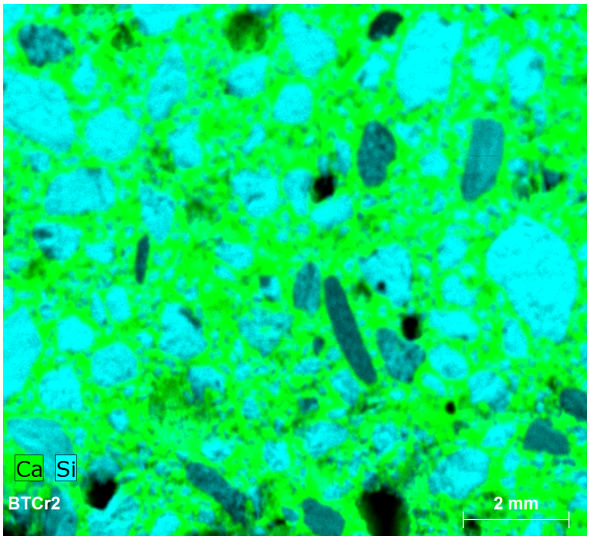

Figure 19: Elemental mapping of sample M 0.5-4.0 with several air bubbles shown as black areas. The dimensions of the image are 10x11 mm.

The Ca-Si-map gave a visually better differentiation of the phases than the S-Ca-Si-map and was therefore chosen as the basis of differentiation for all mortar samples. The CPS of chlorine were retrieved from the spectrum of the cement paste phase. Table 4.5 shows the $\%Agg_{\mu\text{-}XRF}$

and CPS obtained for each sample. The calculation model (see Chapter 2.5) was applied using the obtained $\%Agg_{\mu\text{-XRF}}$ and CPS.

Table 4.5: Counts per second of chlorine (CPS) in the cement paste phase and area percentage of aggregates ($\%Agg_{\mu\text{-XRF}}$) based on a calcium-silica-elemental map of the mortar samples.

Sample	$\%Agg_{\mu\text{-XRF}}$	CPS
M-0.5-0.0	38.2 %	1.15
M-0.5-0.4	38.2 %	3.90
M-0.5-1.5	43.9 %	14.5
M-0.5-4.0	35.1 %	39.3

4.4 Effect of storage of cement paste samples

If the method of determining chloride content by µ-XRF is to be used on concrete samples from real structures, the effect of storage on the measured counts per second (CPS) has to be studied. By doing so, the proper storage of samples prior to analysis can be established. The types of storages examined in this study is storage in isopropanol and storage on a desk.

4.4.1 Storage in isopropanol

An elemental mapping of paste samples stored in isopropanol was taken and the counts per second (CPS) of chlorine using the object-function were measured (see Figure 5). Prior to the elemental mapping, the sample series with a w/c-ratio of 0.4 and 0.6 had been stored in isopropanol for 6 and 2.5 months respectively. The measurements were performed twice to determine the precision of the decimals. The measured CPS before and after storage in isopropanol for sample series with w/c-ratio of 0.4 and 0.6 are shown in Figure 20 and Figure 21, respectively.

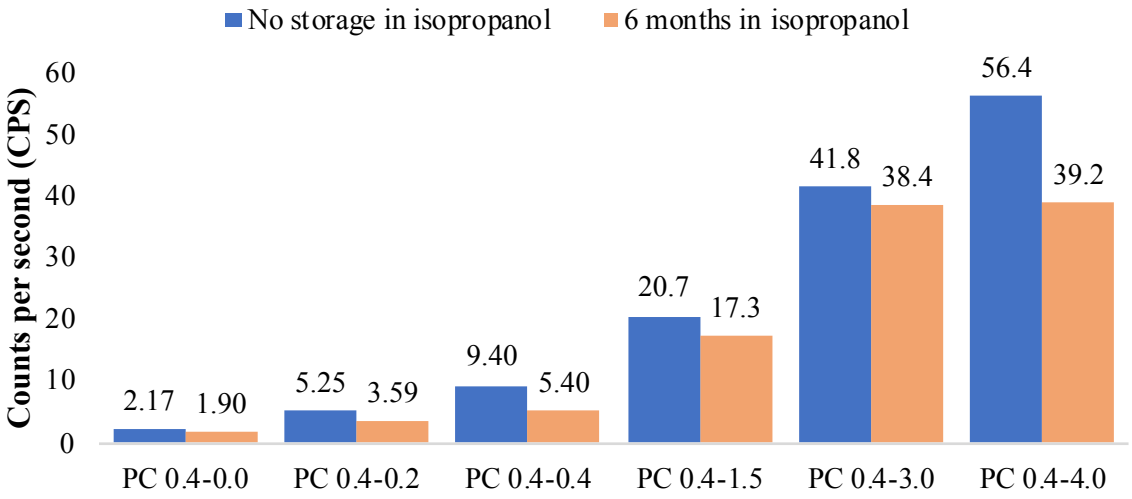

Figure 20: Counts per second of paste samples with w/c = 0.4 before storage in isopropanol (blue) and after six months storage in isopropanol (orange).

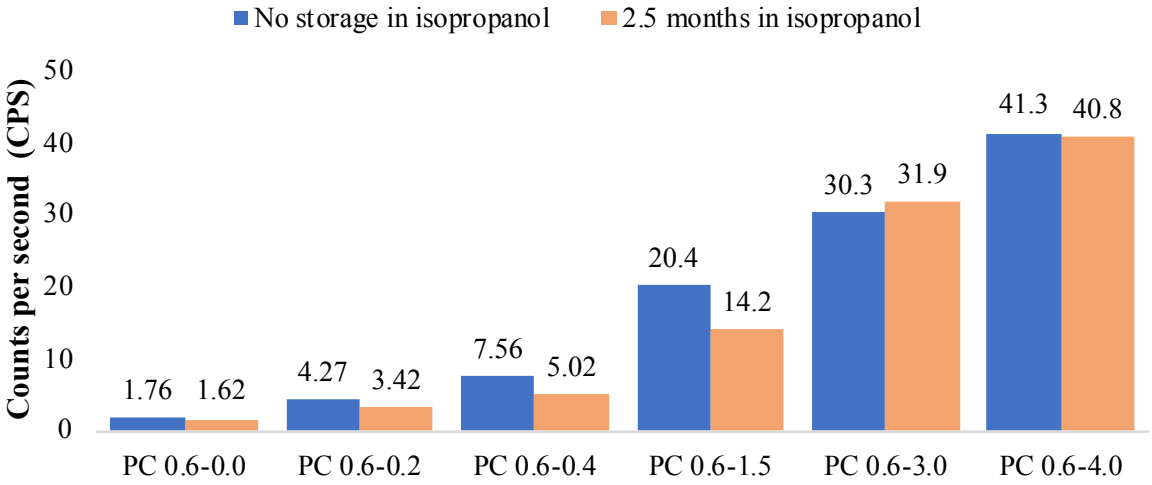

Figure 21: Counts per second of paste samples with w/c = 0.6 before storage in isopropanol (blue) and after two and a half months storage in isopropanol (orange).

The percentage of difference in CPS from before and after storage in isopropanol is shown in Table 4.6. A positive percentage of difference indicates a decrease in CPS and a negative percentage of difference indicates an increase in CPS after storage in isopropanol. The CPS decreases for all samples except for sample PC 0.6-3.0. There does not seem to be any correlation between the percentages of difference in CPS of the samples.

Table 4.6: Percentage of difference in counts per second of chlorine (CPS) before and after storage in isopropanol.

Sample	Percentage difference
PC 0.4-0.0	13 %
PC 0.4-0.2	32 %
PC 0.4-0.4	43 %
PC 0.4-1.5	16 %
PC 0.4-3.0	8 %
PC 0.4-4.0	31 %
PC 0.6-0.0	8 %
PC 0.6-0.2	20 %
PC 0.6-0.4	34 %
PC 0.6-1.5	30 %
PC 0.6-3.0	-5 %
PC 0.6-4.0	1 %

4.4.2 Storage on desk

An elemental mapping of paste samples exposed to air on a desk in the laboratory was taken and the CPS of chlorine using the object-function were measured. The measurements were performed twice to determine the precision of the decimals. Prior to the elemental mapping, all of the analysed samples had been stored on the desk for 10 weeks. The measured CPS before and after storage on the desk are shown in Figure 22.

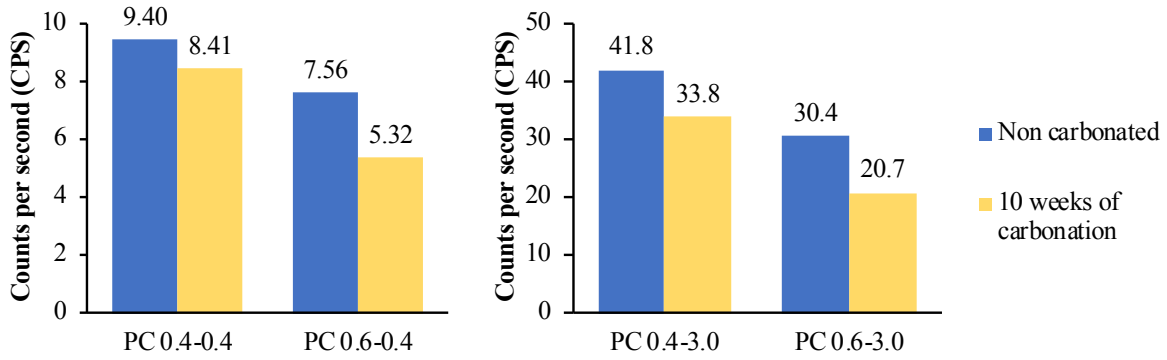

Figure 22: Counts per second of paste samples PC 0.4-0.4 and PC 0.6-0.4 (left) and samples PC 0.4-3.0 and PC 0.6-3.0 (right) before and after storage on desk.

The percentage of decrease in CPS before and after storage on the desk of all samples is shown in Table 4.7. For all samples, the CPS decreased after storage on the desk. The decreases observed for samples PC 0.4-0.4 and PC 0.4-3.0 are similar and likewise for samples PC 0.6-0.4 and PC 0.6-3.0.

Table 4.7: Percentage of difference in CPS of chlorine before and after exposure to air.

Sample	**Percentage difference**
PC 0.4-0.4	11 %
PC 0.6-0.4	30 %
PC 0.4-3.0	19 %
PC 0.6-3.0	32 %

5 Discussion

5.1 Preparation of calibration samples

The intended chloride content of the paste samples based on the added chlorides in the recipe was found to vary from the actual chloride content determined by titration, see Figure 12. Possible reasons for these differences are discussed in the bullet points below:

- The sodium chloride (NaCl) was not dried prior to making the NaCl solutions. However, the water content of the NaCl is thought to be very low compared to the pure water added to mix. Considering the maximum difference of 0.37 % Cl by weight of cement (bwoc), it is unlikely that the water content in the NaCl is the governing reason for the difference in intended and measured chloride content.

- Two different NaCl solutions were used to add chlorides to the samples which could be a reason for the deviations in chloride content. Samples PC 0.4-3.0 and PC 0.4-4.0 have both been mixed with 21.1 wt-% NaCl, yet the difference is large for PC 0.4-3.0 (0.39 % Cl bwoc) and small for PC 0.4-4.0 (0.06 % Cl bwoc). Consequently, there does not seem to be any systematic error correlated with the use of the two NaCl solutions.

- During the mixing, some liquid may have splashed to the roof of the container and thus lowering the amount of chlorides in the mix. As the mixing procedure was the same for all samples, the difference in PC 0.4-4.0 would be larger if this was the reason for the deviations.

- The samples with relatively high amount of chlorides, i.e. above 2.0 % Cl bwoc, are the samples with the largest deviations in chloride content, except for sample PC 0.4-4.0. During the preparation of the calibration samples, accelerated setting occurred when mixing cement paste with a high chloride content. When mixing a paste with a theoretical chloride content of 5%, the consistency was clay-like. The samples with the largest differences in chloride content (PC 0.4-3.0, PC 0.6-3.0 and PC 0.6-4.0) are also the samples which could be affected by accelerated setting. It is possible that this method of mixing cement paste with a high amount of chlorides is the reason for the deviations in intended and measured chloride content.

To summarize, it is hard to identify the reason of the differences in actual and intended chloride content as the mixing procedure and materials were the same for all samples. Even though there are deviations, the reliability index of 0.98 when plotting the actual chloride content versus the intended chloride content (see Figure 13) indicate that the deviations are not significant. However, this method of preparing calibration samples should be followed by a titration to precisely determine the chloride content.

5.2 Comparison of chloride content in cement paste samples determined by titration and by micro X-Ray fluorescence (µ-XRF)

The chloride content of the paste samples determined by micro X-Ray fluorescence (µ-XRF) was plotted as a function of the chloride content determined by titration in Figure 16. In the plot, the trend line for the samples with w/c-ratio of 0.4 had a slightly steeper slope than the trend line for the samples with w/c-ratio of 0.6. This might be due to air bubbles or the inhomogeneity of the samples with a high chloride content which appeared in the elemental

mapping (see Figure 15). If the measurement location coincides with an air bubble, this could affect the CPS in the µ-XRF measurements.

Another possible reason for the difference of the curves is matrix effects as the samples had different w/c-ratios. The particles in the paste samples with w/c-ratio of 0.6 will be further apart than the in the samples with w/c-ratio of 0.4, i.e. the density decreases with increasing w/c-ratio [21]. A material with lower density will absorb more X-Rays and as a consequence more photons will be emitted. A radiation physicist should be consulted to properly understand if and why the density of the paste may have an effect on the µ-XRF measurements.

When looking at the curves in a range closer to the critical chloride content, the difference between the curves is less. Figure 23 shows the trend lines and their equations in the range of 0.0 to 1.2% Cl by weight of cement paste.

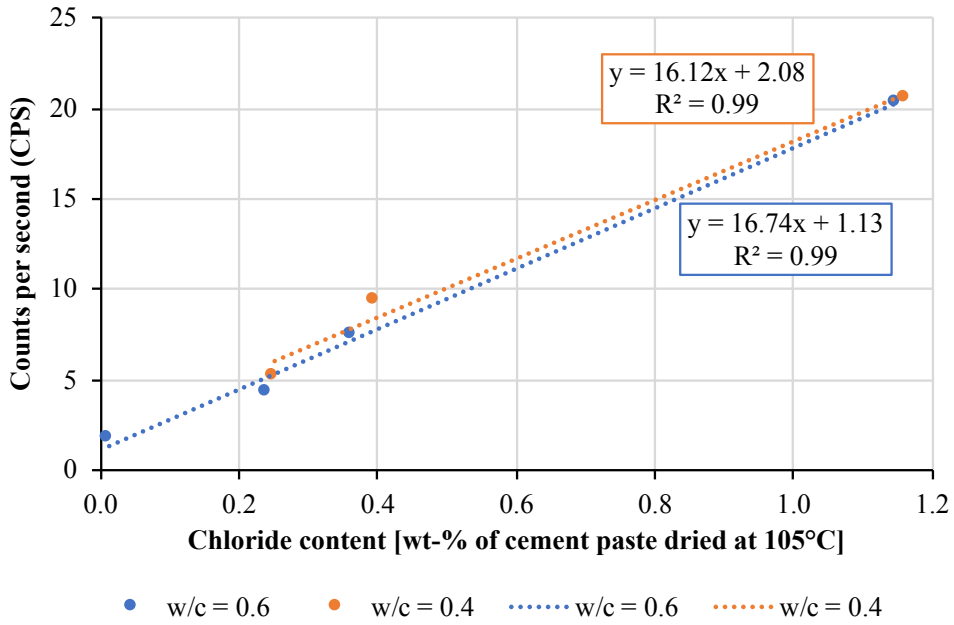

Figure 23: CPS as a function of the chloride (Cl) content of dried cement at 105 °C for cement paste samples with w/c = 0.4 and w/c = 0.6 in the range from 0.0 % Cl to 1.2 % Cl.

In the range from 0.0 to 1.2 % Cl, the two trend lines are close to equal. Using the equations of these calibration curves, the difference in chloride content is approx. 0.04 wt-% of cement paste for a CPS of 10. In this range, the CPS can be considered as independent of the water-to-cement ratio.

The low chloride content in sample PC 0.4-4.0 was quantified in CPS by the µ-XRF whereas the chloride content was too low (less than 0.005 wt-% of cement paste) to be precisely determined by the normal titration procedure. Therefore, the µ-XRF has a lower detection limit for chlorides than titration. Knowing the problem of the detection limit of titration, the volume of filtrate used in the titration was increased for sample PC 0.6-0.0 as previously mentioned. This resulted in a precise determination of chloride content. Without knowing whether the chloride content of a sample is lower than the detection limit of the normal titration procedure, it is necessary to perform the titration twice in order to determine low chloride contents. Once to determine that it is lower than 0.005 wt-% of cement paste and a second time to increase the volume of filtrate to precisely determine the chloride content. In this regard, the low detection limit of µ-XRF is preferable.

As the chloride content determined by titration of reference sample PC 0.6-0.0 was valid, the trend line of the sample series with w/c-ratio of 0.6 in Figure 23 will be used as the calibration curve in further determination of chloride content with µ-XRF. The impact of the choice of calibration curve with regards to determining the chloride content for concrete cores from real structures, will be discussed in a subsequent chapter.

5.3 Phase differentiation

Chloride ions from the environment will be transported through the pore water in the cement paste and the risk of corrosion is mainly dependent on the chloride content in the paste [21]. Therefore, the chloride content of the cement paste is of interest. If the method established in this study is to be used to analyse the chloride content of concrete samples, the aggregates and the cement paste will have to be separated. By doing so, the counts per second (CPS) of chlorine of the cement paste alone, are obtainable. The calibration curve can then be used to determine the chloride content by weight of cement paste.

The phase differentiation of the layers and of the entire surface of concrete sample 2-T-2 in Figure 17 revealed an effect of the collection time and step width of the mapping. Those parameters were the only differences between the two mappings. This effect is not surprising as an increase in collection time will increase the detection of minor element peaks in the spectrum of the analysed pixels. Since the spectrum is the basis for the differentiation, an increase in collection time will give a mapping that retrieves more information about the chemical components of the sample and a better differentiation of the phases. Generally, a decrease in step width will increase the number of analysed pixels and the area with information of the chemical composition of the mapping increases [23]. Which will give a better foundation of information for the phase differentiation.

The differentiation is based on the elements chosen in the elemental mapping. Therefore, the chosen elements will also affect the area percentage of aggregates obtained. This effect will be illustrated by applying the calculation model on a concrete sample using the area percentage of aggregates obtained by different elemental maps in Chapter 5.5.

5.4 Application of the calculation model on mortar samples

To relate the CPs of chlorine of the paste samples determined by µ-XRF to the chloride content by weight of mortar ($\%Cl_{mort\ \mu\text{-}XRF}$), the calculation model was applied on the µ-XRF measurements of the mortar samples. Replacing $\%Cl_{conc\ \mu\text{-}XRF}$ in Equation 8 established in Chapter 2.5 with $\%Cl_{mort\ \mu\text{-}XRF}$ does not change the equation as the mortar samples contain sand. The calculation model for calculating the chloride content by weight of mortar can be expressed as:

$$\%Cl_{mort\ \mu-XRF} = \%Cl_{paste\ \mu-XRF} \cdot \frac{\rho_{paste} \cdot \left(1 - \%Agg_{\mu-XRF}\right)}{\rho_{agg} \cdot \%Agg_{\mu-XRF} + \rho_{paste} \cdot \left(1 - \%Agg_{\mu-XRF}\right)} \quad (10)$$

With ρ_{agg} the density of aggregates assumed to be 2700 kg/m^3. $\%Cl_{paste\ \mu\text{-}XRF}$ was established by the calibration curve of the cement paste samples with w/c-ratio of 0.6, see Figure 23.

The aggregate and cement paste phases of sample M 0.5-1.5 based on a S-Ca-Si-map and a Ca-Si-map are shown in Figure 18. Different area percentage of aggregates ($\%Agg_{\mu\text{-}XRF}$) were obtained by differentiation of the two elemental maps. For both elemental maps, the calculation model was applied using the CPS of chlorine in the paste and $\%Agg_{\mu\text{-}XRF}$. The resulting chloride content was 0.42 wt-% of mortar for the S-Ca-Si-map and 0.37 wt-% of mortar for the Ca-Si-map. A difference of 0.05% Cl by weight of mortar is significant when comparing with the critical limit of 0.07% Cl by weight of concrete. Consequently, the choice of elements as the basis for the elemental mapping has an influence on the differentiation of the mortar samples.

The Ca-Si-map was chosen as the basis of the differentiation for all mortar samples, as it gave a visually better differentiation. The chloride content determined by the calculation model was plotted as a function of the chloride content determined by titration of the mortar when dried at 105°C, see Figure 24. The uncertainties of the chloride content determined by titration are excluded as they were too small to be visible in the plot.

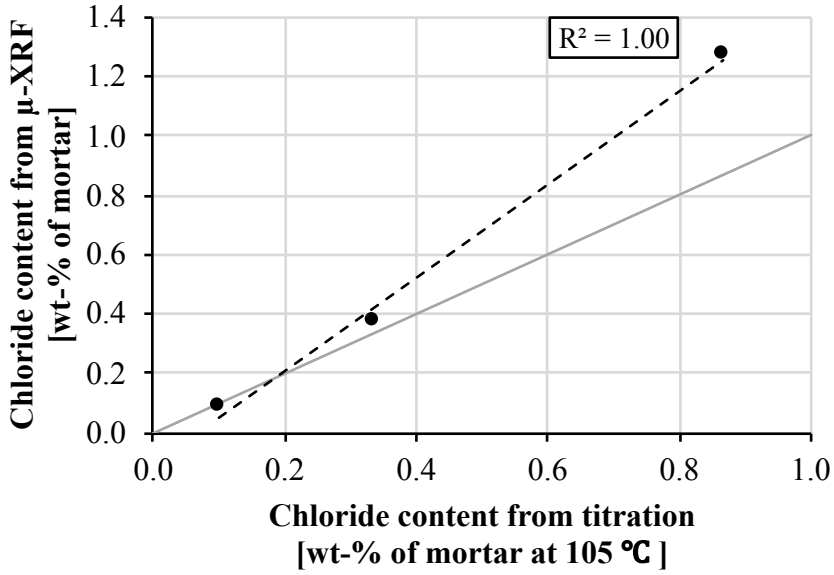

Figure 24: Chloride content of mortar samples M 0.5-0.4, M 0.5-1.5 and M 0.5-4.0 by weight of concrete determined by titration versus the chloride content determined by µ-XRF and application of the established model. The grey line represents a 1:1 ratio

The samples with a low chloride content i.e. M 0.5-0.4 and M 0.5-1.5 lie close to the grey line representing the 1:1 ratio, whereas sample M 0.5-4.0 lies significantly above. A possible reason for the deviation could be the air bubbles observed in sample M 0.5-4.0 which can affect the µ-XRF measurements. Moreover, bleeding of sample M 0.5-4.0 was observed which could lower the w/c-ratio and change the morphology. The effect of the morphology on µ-XRF measurements should be studied further.

Furthermore, different settings were used due to the time limit for mappings in the M4 Tornado software. The mappings were taken with a collection time of 5 ms per pixel and step widths of 10 µm while the collection time and step width of the mapping of the cement paste samples were 1 ms per pixel and 35 µm. This could have an effect when applying the calibration curve which is based on the measurements of the cement paste samples. A way to increase the time limit of mappings in M4 Tornado ought to be found since the mappings should performed with the same settings.

5.5 Application of the calculation model on concrete samples

In order to determine the effect of the elements chosen as basis for the differentiation of phases, the area percentage of aggregates ($\%Agg_{\mu\text{-}XRF}$) retrieved from different elemental maps was tested with the calculation model. $\%Agg_{\mu\text{-}XRF}$ was retrieved from a sulphur-calcium-silica-elemental map (S-Ca-Si-map), a sulphur-calcium-elemental map (S-Ca-map) and a sulphur-elemental map (S-map). The chloride content of the layers in sample 2-T-2 was determined by the calculation model using the $\%Agg_{\mu\text{-}XRF}$ and CPS of chlorine from the three elemental maps. The chloride content determined by titration and the chloride content determined by the three elemental maps were plotted as a function of the depth of sample 2-T-2, see Figure 25. The exact values of the plot can be found in Appendix A.8.

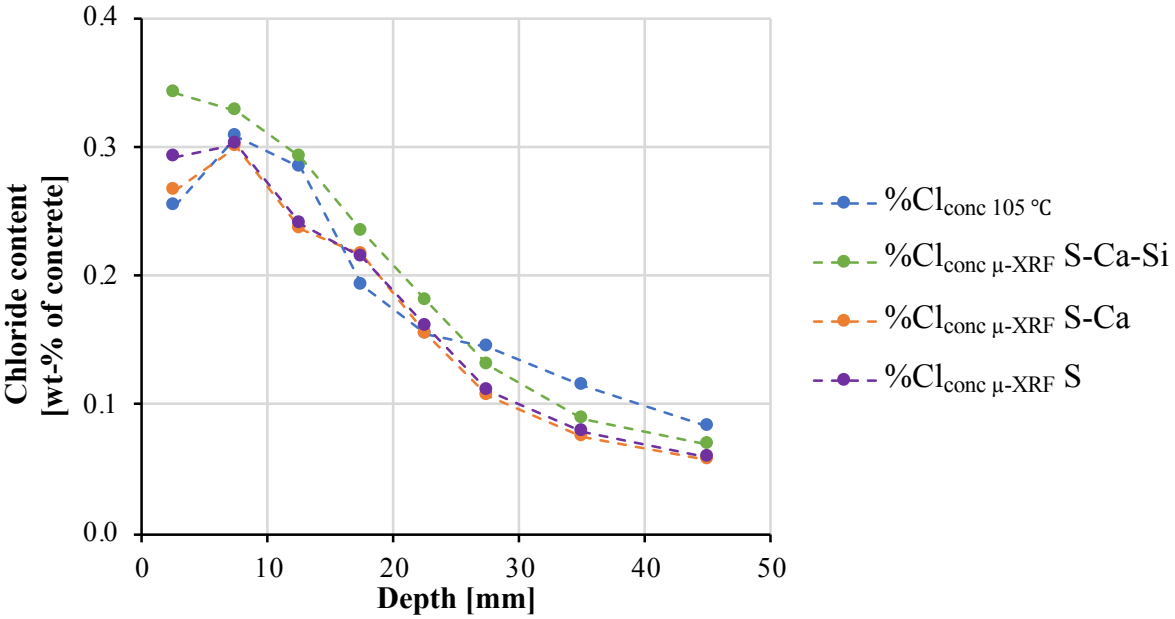

Figure 25: Chloride content of sample 2-T-2 by weight of concrete determined by titration $\%Cl_{conc\ 105\ °C}$ (blue) and by use of the calculation model based on sulphur-calcium-silica-elemental map ($\%Cl_{conc\ \mu\text{-}XRF}$ S-Ca-Si), sulphur-calcium-elemental map ($\%Cl_{conc\ \mu\text{-}XRF}$ S-Ca) and a sulphur-elemental map ($\%Cl_{conc\ \mu\text{-}XRF}$ S).

The difference between the chloride (Cl) content determined by different elemental maps is largest in the outermost layers of the sample. The largest difference of 0.08% Cl by weight of concrete is between the S-Ca-Si-map and the S-Ca-map in layer 0-5 mm. When reaching layer 15-20 mm, the chloride profiles are approximately parallel, and the largest difference is 0.03 wt-% of concrete, also between the S-Ca-Si-map and S-Ca-map. This indicates that the effect of the choice of elements in the mapping is minor deeper in the concrete sample. However, this contradicts the results of the mortar samples where the choice of elements had an effect on the differentiation.

The main differences between the mortar and concrete samples are the size of the aggregates, the step width and the area of the mappings. Larger aggregates may be easier to detect for the µ-XRF and could be a reason for improved results for the concrete samples compared to the mortar samples.

Furthermore, the mapping of the mortar samples became pixelated due to the small area as previously mentioned. The minimum area of the mapping of the layers in sample 2-T-2, was 90x5 mm whereas the area of the mapping of the mortar samples was 10x11 mm. It is possible

that the pixelated mappings could affect the phase differentiation. Additionally, the step width of the mapping of the mortar samples was reduced from 35 µm to 10 µm due to the pixelated mapping, while a step width of 35 µm for sample 2-T-2 gave a good resolution of the mapping. The difference in step width and area of the mapping seem to influence the resolution of the mapping and therefore the differentiation of the phases.

The calculation model was also tested with the volume percentage of aggregates based on the recipe ($\%Agg_{recipe}$). The area percentage of aggregates and the counts per second (CPS) are both retrieved from µ-XRF. To avoid additional errors, the calculation model should be applied on the chloride content from titration to test the effect of $\%Agg_{recipe}$. In order to accomplish this, the calculation model has to be reversed and the chloride concentration determined by the calibration curve has to be replaced with the concentrations obtained from titration. By doing so the concentration can be related from wt-% of concrete to wt-% of cement paste. The chloride content per mass cement paste based on the titration results can then be expressed as:

$$\%Cl_{paste\ 105\,℃} = \%Cl_{conc\ 105°C} \cdot \frac{\rho_{agg} \cdot \%Agg_{recipe} + \rho_{paste} \cdot (1 - \%Agg_{recipe})}{\rho_{paste} \cdot (1 - \%Agg_{recipe})} \quad (9)$$

With $\%Cl_{conc\ 105°C}$ the chloride content per mass concrete determined by titration and $\%Agg_{recipe}$ the volume percentage of aggregates based on the added amounts in the recipe.

The chloride content by weight of cement paste was also determined by application of the calibration curve ($\%Cl_{paste\ µ\text{-}XRF}$). The chloride content by weight of cement paste determined by the calibration curve and by titration in each layer of sample 2-T-2 is plotted in Figure 26.

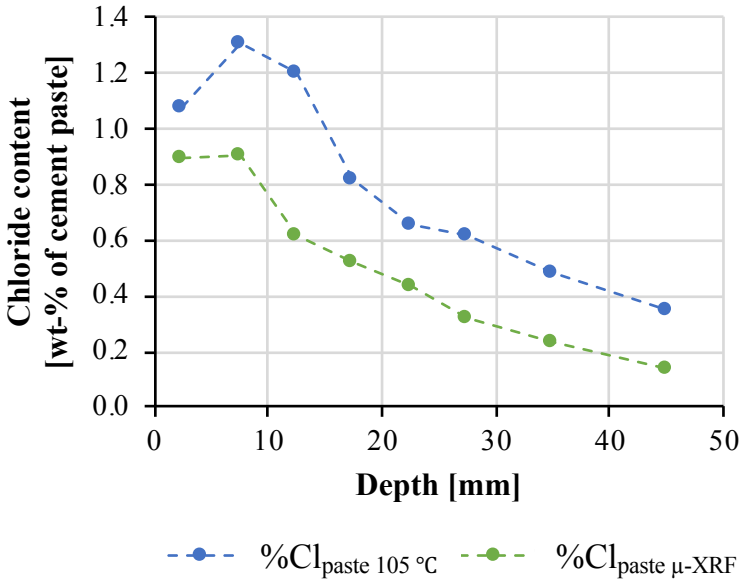

Figure 26: Chloride content by weight of cement paste determined by titration $\%Cl_{paste}$ 105 ℃ (blue) and by use of the calibration curve $\%Cl_{paste\ µ\text{-}XRF}$ (green) for concrete sample 2-T-2.

When applying the reversed calculation model with $\%Agg_{recipe}$, the chloride content determined by titration is above that determined by µ-XRF in every layer. For all layers, the maximum difference in chloride content is 0.58 wt-% of cement paste. The fact that there is no scatter above and below the chloride concentration from titration, indicates a systematic error. This is logical as it is unlikely that the volume percentage of aggregates is constant in every layer and

the theoretical concrete recipe is often slightly different than that of the cast concrete. Further, $\%Agg_{recipe}$ is based on the amounts in the recipe while $\%Agg_{\mu\text{-XRF}}$ is based on µ-XRF and has the same basis as the CPS.

Having established the preferable parameters for the model, $\%Agg_{\mu\text{-XRF}}$ based on S-Ca-Si-maps was retrieved for all concrete samples. Using $\%Agg_{\mu\text{-XRF}}$, the chloride content of the layers was determined by application of the calculation model. The chloride content from the calculation model ($\%Cl_{conc\ \mu\text{-XRF}}$) and that determined by titration ($\%Cl_{conc\ 105\ °C}$) in each layer were plotted as a function of the depth of the concrete cores, see Figure 27. The exact values of calculation can be found in Appendix A.9.

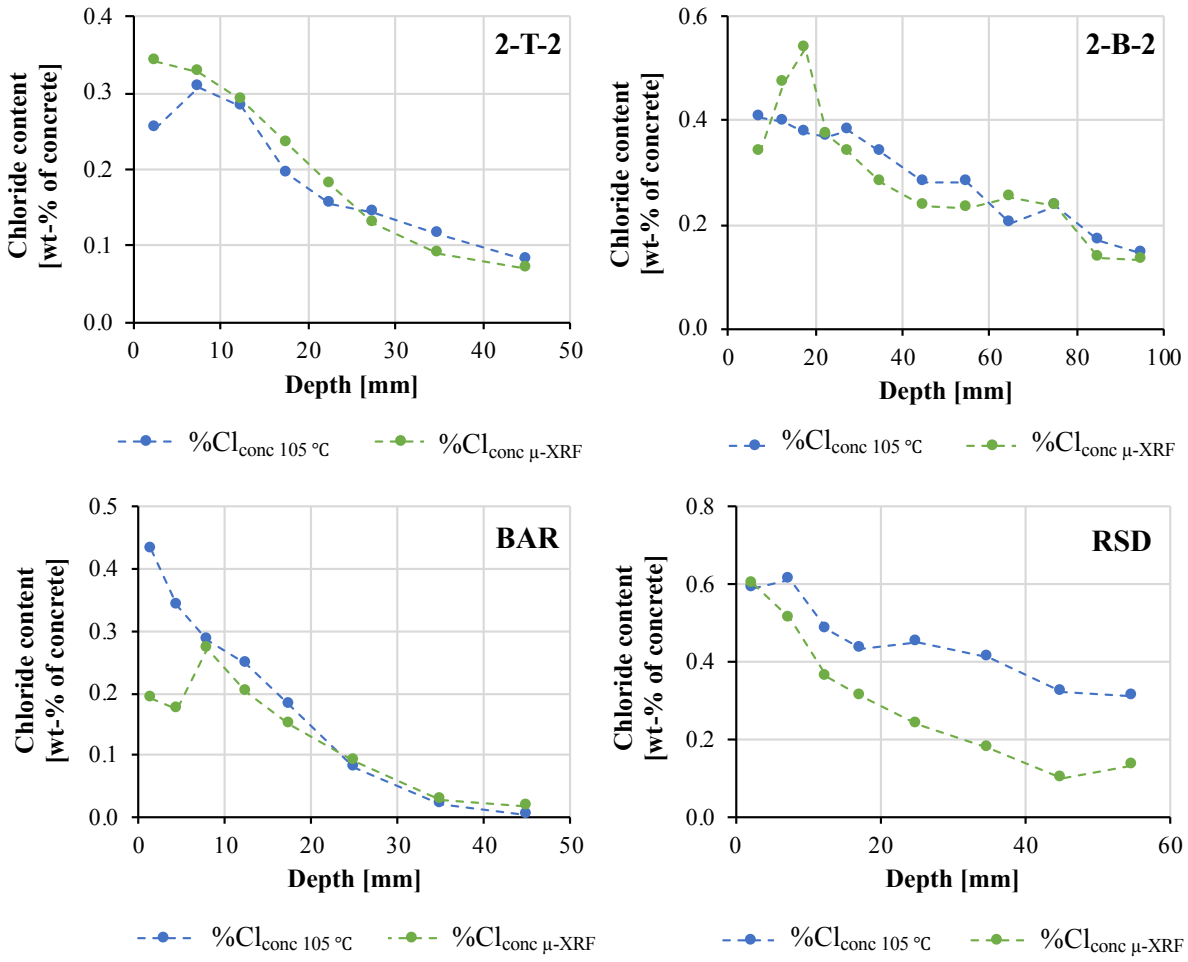

Figure 27: Chloride content by weight of concrete determined by titration (blue) and by use of the established model (green) for concrete samples 2-T-2 (top left), 2-B-2 (top right), BAR (bottom left) and RSD (bottom right).

When excluding the results for sample RSD, $\%Cl_{conc\ \mu\text{-XRF}}$ in the outermost layers (0-10 mm) differ the most from $\%Cl_{conc\ 105\ °C}$. The maximum differences between $\%Cl_{conc\ \mu\text{-XRF}}$ and $\%Cl_{conc\ 105\ °C}$ in the layers are given in Table 5.1.

Table 5.1: Maximum difference between the chloride contents determined by the calculation model ($\%Cl_{conc\ \mu\text{-}XRF}$) and by titration ($\%Cl_{conc\ 105\ °C}$) for concrete samples. All concentrations are given by weight of concrete.

	Maximum difference between $\%Cl_{conc\ \mu\text{-}XRF}$ and $\%Cl_{conc\ 105\ °C}$			
Depth	**2-T-2**	**2-B-2**	**BAR**	**RSD**
0 to 20 mm	0.63 %	0.09 %	-0.24 %	-0.12 %
20 mm to maximum depth of core	±0.03 %	-0.06 %	0.01 %	-0.23 %

Except for sample RSD, the maximum difference in chloride content is in a layer less than 20 mm from the surface. The higher w/c-ratio and different morphology in the layers close to the surface of the concrete created by the wall effect [16] may have an effect on the μ-XRF measurements. Therefore, variations in the outer layers are not unexpected. In the layers beyond 20 mm, the difference in chloride content is less. However, the maximum differences are relatively high when comparing with the critical limit 0.07 wt-% of concrete. Determined by titration, sample BAR has a chloride content of 0.05 wt-% of concrete in layer 40-50 mm which is less than the critical chloride concentration by weight of concrete 0.07 % [5]. The chloride content from the calculation model in this layer is also 0.05 wt-% of concrete. In consequence, the method of chloride content determination by μ-XRF is able to detect concentrations below the critical limit of chloride concentration. Furthermore, the two chloride profiles of sample BAR are close to equal below 0.1 % Cl by weight of concrete. It is the low chloride contents (less than 0.1 % Cl) that are of interest when determining if there is a risk of reinforcement corrosion.

The fact that $\%Cl_{conc\ \mu\text{-}XRF}$ is scattered above and below $\%Cl_{conc\ 105\ °C}$ suggests that the method has a good accuracy. Knowing that the chloride content per concrete mass determined by the calculation model does not differ substantially from the determination from titration, the method can be applied for estimating the chloride content in concrete. Further, the small differences in chloride content determined by μ-XRF and by titration in sample BAR, indicate that the method can be applied for determining chloride contents below the critical chloride limit with good accuracy.

As for the mortar samples, the collection time of the mappings of the layers (5 ms per pixel) was different from that of the cement paste samples (1 ms per pixel) and therefore different from the basis of the calibration curve. This was due restraints caused by the software and hardware used, as a mapping can maximum take 2 hours to finish. As previously mentioned, a way to increase the time limit of mappings in M4 Tornado ought to be found since the mappings should performed with the same settings.

5.5.1 Sensitivity analysis of the calculation model

A sensitivity analysis of the calculation model was performed for all concrete samples with regard to the area percentage of aggregates ($\%Agg_{\mu\text{-}XRF}$) and the slope of the calibration curve. The $\%Agg_{\mu\text{-}XRF}$ and the slope of the calibration curve were individually increased and decreased by 15%. Subsequent to each change, the difference in chloride content determined by μ-XRF and by titration in each layer was calculated. The outer layers (0-10 mm) of the concrete samples were excluded from the analysis due to the varying results most likley due to morphology effects.

The absolute values of the differences were taken. Subsequently, the absolute values were averaged and thus obtaining the average absolute difference in chloride content. The average absolute differences in each the layers were used to compare the effect of changes in $\%Agg_{\mu\text{-}XRF}$ and the slope to the original average absolute differences. Refer to Appendix A.10 for details of the sensitivity analysis. The effect of a 15 % increase and decrease in $\%Agg_{\mu\text{-}XRF}$ and slope on the average absolute difference in chloride content is shown in Figure 28.

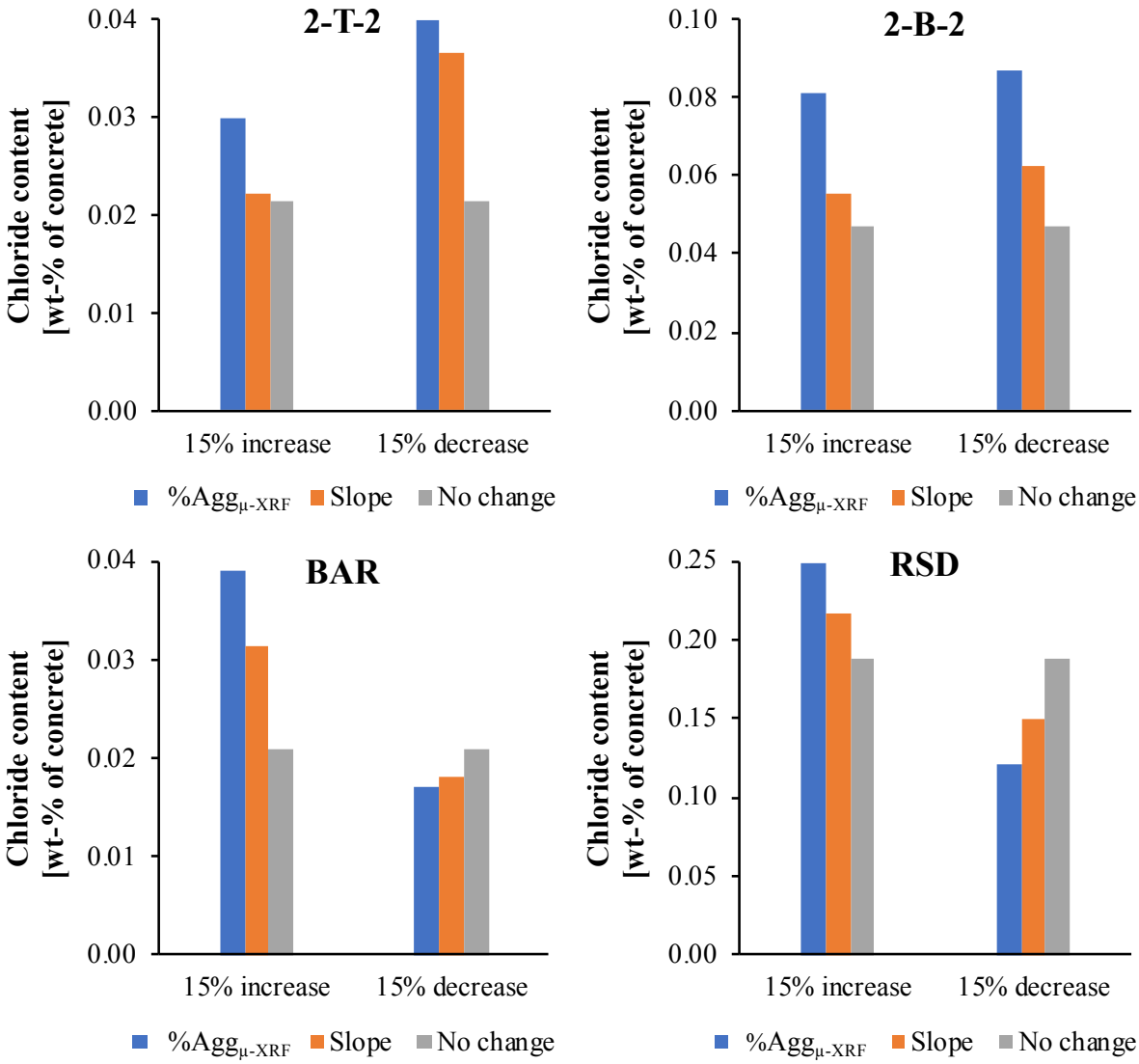

Figure 28: Average absolute difference in chloride content by weight of concrete for samples 2-T-2, 2-B-2, RSD and BAR when the area percentage of aggregates ($\%Agg_{\mu\text{-}XRF}$) and the slope of the calibration curve have been individually increased and decreased by 15%. The differences are compared to the average absolute difference without alteration in $\%Agg_{\mu\text{-}XRF}$ and slope.

Generally, the sensitivity analysis reveals that the model is more sensitive to a change of the area percentage of aggregates than a change in the slope of the calibration curve. In addition, it is observed that the if the average absolute difference decreases when the slope is changed then it will also decrease when $\%Agg_{\mu\text{-}XRF}$ is changed by the same percentage and vice versa. Due to the models sensitivity to the area percentage of aggregates more information regarding the background of the creation of the phases should be gained.

5.6 Storage of samples

Four paste samples with varying w/c-ratios and chloride concentrations were stored on a desk. The measured CPS of the samples with a w/c-ratio of 0.4 have decreased less than the samples with a w/c-ratio of 0.6 as observed from Figure 22. This was observed regardless of the chloride concentration. The samples with a w/c-ratio of 0.6 will have a lower density than the samples with a w/c-ratio of 0.4. This indicates that the density of the cement paste may affect the CPS when exposed to air. Cementitious materials exposed to humidity and oxygen will at the right conditions carbonate. The rate of carbonation increases with decreasing density as pastes with a low density will be more permeable [21]. Considering this, it is likely that carbonation effects the µ-XRF measurements of cement paste.

A decrease in CPS was also observed for the samples stored in isopropanol. It is possible that the chlorides in the samples may have leached out into the isopropanol. To confirm or refute this hypothesis, a titration to determine the chloride content of the isopropanol should be performed.

5.7 Choice of µ-XRF measurement types and effect of the µ-XRF parameters

Since the paste samples with a high chloride content seem to be inhomogeneous, an average of the CPS of the entire sample is preferable. Performing several point measurements is possible, however the amount of measurement points has to be high to achieve a good statistical background. Setting the sample time of each point measurement to e.g. 15 seconds and having a high amount of points will result in a time-consuming process. Furthermore, this process has to be repeated for each sample. Another option is to use the elemental mapping of the samples to obtain an average for each sample by utilizing the object-function in the M4 Tornado software. The surface of the sample in the elemental mapping is marked and the spectrum of the entire sample is retrieved directly. The elemental mapping can take several hours to finish, on the other hand one can leave the measurement to finish without supervising it. By using the elemental mapping and the object-function, one can obtain an average with a better statistical background with less time in the lab.

Further, the beam current and the number of detectors with which the mapping of a sample is taken has an effect on the CPS obtained. A higher beam current will excite electrons with a higher energy binding it to its orbit and more photons will be emitted, increasing the CPS. Moreover, a higher number of detectors will increase of the number photons detected and therefore increase the CPS.

5.8 Sources of error

In addition to the previously mentioned possible error sources of the established calculation model, other error sources were detected in features of the M4 Tornado software.

When marking the area of interest of the concrete samples for elemental mapping, a certain area near the surface of the sample was excluded. Any area of the mapping which included the sample table was differentiated as a part of the aggregate phase and thus influencing the area percentage of aggregates. As the surface of the concrete was slightly irregular, it was necessary to exclude some area of the sample to obtain an area percentage of aggregate which was not influenced by the sample table. An example of a phase differentiation that includes an area around the samples is shown in Figure 29.

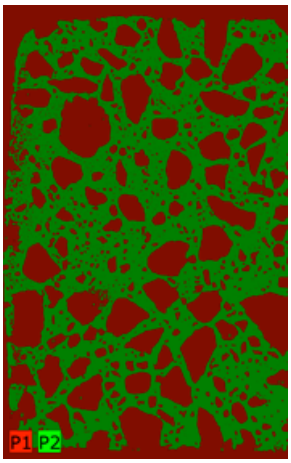

Figure 29: Phase differentiation of sample 2-T-2 when an area around the sample is included. The red area is the aggregate phase and the green area is the cement paste phase.

The precision of the marking of layers in the elemental mapping is also a possible source of error. The width of the layers is the same as the depths intervals which are profile ground and analysed by titration. However, since some of the area of the irregular surface of the sample is excluded, it is possible that the layers of the mapping are not equal to the depth intervals analysed by titration. Due to this, the intervals of the profile grounding and the layers of the mapping may overlap. In addition, the volume for the determination of chloride content by μ-XRF and the volume for the determination by titration are of very different sizes. For titration, one half of the concrete core was profile ground and the concrete powder at different depth intervals was analysed. Whereas the penetration depth of the X-Ray beam into a sample is only approx. 2 mm [9]. The chloride content determined by μ-XRF is based on smaller volume and therefore a volume that is less representative than the volume of sample analysed by titration.

6 Conclusion

We were able to cast cement paste for calibration, however we encountered challenges with accelerated setting when the chloride content was too high (approx. 5 wt-%). The high chloride content resulted in inhomogeneities of the chloride content distribution. In addition, the method of mixing the samples created air bubbles in the samples. The intended chloride concentrations based on the added chlorides in the recipe were different from the chloride contents determined by titration, therefore the cement paste samples should be titrated to determine the exact amount of chloride mass.

A linear relation was obtained between the CPS values determined by the µ-XRF and the chloride content per cement paste mass obtained by titration. Additionally, this relation was found to be independent of the water-to-cement ratio in the range or 0.0 to 1.2% chlorides per mass cement paste. The relation can be used for calibration of µ-XRF measurements i.e. transferring CPS values to chloride content per cement paste mass for similar samples. The detection limit for chlorides of the µ-XRF was found to be lower than that of the potentiometric titration.

The object-function of the M4 Tornado was evaluated to be good for measuring the counts per second of a sample as it gives an average for the whole area. Carbonation and storage in isopropanol were observed to have an effect on the measured counts per second of chlorine in the paste sampled.

The phase function in the M4 Tornado software gave a visually adequate differentiation of the cement paste and aggregates. An effect was observed for the choice of elements in the elemental mapping upon which the differentiation of the aggregate and cement paste phases is based. A technique of estimating the chlorides per mass concrete was established by applying the calibration curve and the area percentage of aggregates attained by the phase function in the M4 Tornado. The technique was found to give chloride contents comparable with potentiometric titration and gave the best results at a depth beyond 20 mm in concrete cores. Sample RSD gave deviating results compared to the other samples. The technique was found have high accuracy for determining chloride contents below the critical chloride content threshold per mass concrete. The collection time and step width of the µ-XRF mapping was discovered to have a possible effect on the estimation of chloride concentration.

A sensitivity analysis revealed that the technique is more sensitive to a change in area percentage of aggregates than the slope of the calibration curve.

7 Further work

This study has shown that the experimental work has limitations and can be improved. The results should be extended by further work. Recommendations for further work are as follows:

- One should use volumetric measurements in the preparation of cement and mortar samples with a known chloride content. Air bubbles in the samples could interfere with μ-XRF measurements. It is therefore recommended to use a vacuum mixer which should reduce the amount of air bubbles.
- To determine whether the cement type will have an effect on the μ-XRF measurements, cement paste samples of different cement types should be tested with μ-XRF.
- The titration of sample PC 0.4-0.0 and M 0.5-0.0 should be performed again with an increased volume of filtrate to achieve a valid value of the chloride concentration.
- The effects of parameters such as the collection time and step width on the resolution of μ-XRF mappings and the differentiation of phases should be further investigated. To properly understand and interpret the effects observed, a physicist with knowledge of radiation physics should be consulted.
- The effects of carbonation and storage and isopropanol of cement paste samples should be further examined in order to determine the best method of storage of samples.
- Possible matrix effects should be further investigated.

8 Appendices

8.1 Appendix A.1 – The derivation of the expression for $\%Cl_{conc\ \mu\text{-}XRF}$

The chloride content by weight of concrete can be expressed as:

$$\%Cl_{conc} = \frac{m_{Cl}}{m_{conc}} = \frac{m_{Cl}}{m_{paste}} \cdot \frac{m_{paste}}{m_{conc}} = \frac{m_{Cl}\ [kg]}{m_{paste}\ [kg]} \cdot \frac{\rho_{paste}\ \left[\frac{kg}{m^3}\right] \cdot V_{paste}\ [m^3]}{\rho_{conc}\ \left[\frac{kg}{m^3}\right] \cdot V_{conc}\ [m^3]} \qquad (A1)$$

With m_{Cl} the mass of chlorides, m_{conc} the mass of concrete, m_{paste} the mass of cement paste, ρ_{paste} the density of cement paste, ρ_{conc} the density of concrete, V_{paste} the volume of cement paste and V_{conc} the volume of concrete.

The density of concrete and of cement paste have to be determined to solve equation A1.

The mass of concrete is the sum of the mass of cement paste and aggregates, i.e. $m_{conc} = m_{paste} + m_{agg}$. By expressing the mass as the product of density and volume and rearranging the equation, we can express the density of concrete with the following equation:

$$\rho_{conc} = \frac{m_{agg} + m_{paste}}{V_{conc}} = \rho_{agg} \cdot \frac{V_{agg}}{V_{conc}} + \rho_{paste} \cdot \frac{V_{paste}}{V_{conc}} \qquad (A2)$$

With $V_{agg}\ [m^3]$ the volume of aggregates.

The cement paste is the sum of the mass of water, m_w, and the mass of cement, m_{cem}. Therefore, the density of cement paste can be determined with the following equation:

$$\rho_{paste} = \frac{m_{paste}}{V_{paste}} = \frac{m_w + m_{cem}}{V_w + V_{cem}} = \frac{m_w + m_{cem}}{\frac{m_w}{\rho_w} + \frac{m_{cem}}{\rho_{cem}}} \qquad (A3)$$

By rearranging equation A3, we get:

$$\rho_{paste} = \frac{\rho_w \cdot \rho_{cem} \cdot \left(\frac{w}{c} + 1\right)}{\rho_{cem} \cdot \frac{w}{c} + \rho_w} \qquad (A4)$$

With $\frac{w}{c}$ water-to-cement-ratio i.e. the mass of water divided the mass of cement, ρ_w the density of water and ρ_{cem} the density of cement. The last unknown in equation A1 is now the mass of cement paste divided by the mass of concrete, $\frac{m_{paste}}{m_{conc}}$. By using the expression for ρ_{conc} in equation A2, the ratio can be determined with the following equation:

$$\frac{m_{paste}}{m_{conc}} = \frac{\rho_{paste} \cdot V_{paste}}{\rho_{conc} \cdot V_{conc}} = \frac{\rho_{paste} \cdot \frac{V_{paste}}{V_{conc}}}{\rho_{agg} \cdot \frac{V_{agg}}{V_{conc}} + \rho_{paste} \cdot \frac{V_{paste}}{V_{conc}}} \quad (A5)$$

The amount of chlorides in the cement paste, m_{Cl}/m_{paste}, is determined by a calibration curve with a linear relationship i.e. y = ax + b, where x is equal m_{Cl}/m_{paste}. Then m_{Cl}/m_{paste} can be expressed as:

$$\frac{m_{Cl}}{m_{paste}} = \%Cl_{paste\ \mu-XRF} = ax + b \quad (A6)$$

By rearranging equation A1 and inserting equation A5 and A6, we can determine the chloride content by weight of concrete with the following equation:

$$\%Cl_{conc} = \%Cl_{paste} \cdot \frac{\rho_{paste} \cdot \left(1 - \frac{V_{agg}}{V_{conc}}\right)}{\rho_{agg} \cdot \frac{V_{agg}}{V_{conc}} + \rho_{paste} \cdot \left(1 - \frac{V_{agg}}{V_{conc}}\right)} \quad (A7)$$

The model assumes that volume percentage of aggregates (V_{agg}/V_{conc}) is the same as the area percentage of aggregates ($\%Agg_{\mu-XRF}$) determined by μ-XRF. Therefore, the equation A6 may be rewritten as:

$$\%Cl_{conc\ \mu-XRF} = \%Cl_{paste\ \mu-XRF} \cdot \frac{\rho_{paste} \cdot \left(1 - \%Agg_{\mu-XRF}\right)}{\rho_{agg} \cdot \%Agg_{\mu-XRF} + \rho_{paste} \cdot \left(1 - \%Agg_{\mu-XRF}\right)}$$

With ρ_{paste} as defined in equation A4.

8.2 Appendix A.2 – Cement data provided by Norcem AS

NORCEM
HEIDELBERGCEMENT Group

"FN 19" Laboratoriesement

REPORT ON QUALITY TEST CEM I 52,5 N

Costumer: Date received: Tor Magnus Zackariassen, 21.10.2015
Sample Marked: Uttatt 2000kg på Norviking 20.10.15
Your ref.: 143/15
Our ref.: **EG-2015-0003**

Parameter:		Results:		Method:
CHEMICAL COMPOSITION				
Chemical Parameters				
Free Lime		1.09	%	PD0468
Loss On Ignition	LOI	1.26	%	EN196-2
Sulfur Trioxide-IR	SO3	3.39	%	PD1752
Carbon	C CI	0.07	%	PD1752
Total Chloride	Cr(VI)	0.025	% Cl	EN196-2
Water soluble Chromium	I.R	0.00	mg/kg	EN196-10
Insoluble Residue		0.18	%	EN196-2
XRF Analysis	SiO2			
Silica Oxide	Al2O3	21.12	%	EN196-2
Aluminum Oxide	Fe2O3	4.60	%	EN196-2
Ferric Oxide	CaO	3.77	%	EN196-2
Calsium Oxide	K2O	63.21	%	EN196-2
Potassium Oxide	Na2O	0.40	%	EN196-2
Sodium Oxide	MgO	0.35	%	EN196-2
Magnesium Oxide	TiO2	1.71	%	EN196-2
Titanium Dioxide	P2O5	0.314	%	EN196-2
Phosphorous Pentoxide	Mn2O3	0.182	%	EN196-2
Manganic Oxide	Na2O Eq.	0.059	%	EN196-2
Sodium Oxide Equivalent		0.61	%	EN196-2
TECHNICAL PARAMETERS				
Compressive Strength				
After 1 day		18.4	MPa	EN196-1
After 2 days		30.1	MPa	EN196-1
After 7 days		42.2	MPa	EN196-1
After 28 days		58.0	MPa	EN196-1
Fineness				
Specific surface, Blaine		388	m2/kg	EN196-6
Particle Size Distribution				
Sieve Passing	<24 µm	69.8	%	PD1749
Sieve Passing	<30 µm	78.2	%	PD1749
Sieve Residue	>64 µm	2.9	%	PD1749
Sieve Residue	>90 µm	0.4	%	PD1749
Other Technical Parameters				
False Set		0	min	PD1793
Time of Setting				
Initial		142	min	EN196-3
Soundness				
Le Chatelier		0.0	mm	EN196-3
Normal Consistency				
Temperate climate 20°C		27.9	%	EN196-3

Norcem A.S Brevik, Cement and Concrete Laboratory, 24.11.2015 ~~Laboratory Manager~~

NORCEM AS

Adress: Setreveien 2, P.O. Box 38, N-3991 Brevik
Phone: +47-35-57 20 00
Telefax: +47-35-57 04 00
Ent.no.: NO 934 949145 VAT
Bank Account: 6003 06 12488
Head Office: Lilleakerveien 2b, P.O. Box 143 Lilleaker, 0216 Oslo

8.3 Appendix A.3 – Raw data sodium chloride (NaCl) solution

Table A.3.1: Raw data for recalculation of the concentration in wt-% NaCl of the NaCl solutions

Parameters	25 wt-% NaCl	5 wt-% NaCl
Density at 20°C [kg/L]	1.1887*	1.0340*
Amount NaCl [g]	250	50
Volume NaCl solution [L]	1	1
Weight NaCl solution [kg]	1.1887	1.0340
Concentration [wt-%]	21.0	4.8

*Density of NaCl is taken from the table provided by Mettler Toledo [24]

Table A.3.2: w/c = 0.4

Sample	Cement [g]	Weighed in NaCl solution [g]	Mass NaCl in sample [g]	Mass Cl in sample [g]	%Cl [wt-% of cement]
PC 0.4-0.2	100.00	6.59	0.32	0.19	0.19
PC 0.4-0.4	100.00	13.19	0.64	0.39	0.39
PC 0.4-1.5*	100.00	9.89	2.08	1.26	1.26
PC 0.4-3.0*	100.00	19.78	4.16	2.52	2.52
PC 0.4-4.0*	100.00	26.38	5.55	3.37	3.37

*These samples were mixed with 21.1 wt-% NaCl. The rest were mixed with 4.8 wt-% NaCl.

Table A.3.3: w/c = 0.6

Sample	Cement [g]	Weighed in NaCl solution [g]	Mass NaCl in sample [g]	Mass Cl in sample [g]	%Cl [wt-% of cement]
PC 0.6-0.2	100.00	6.59	0.32	0.19	0.19
PC 0.6-0.4	100.00	13.19	0.64	0.39	0.39
PC 0.6-1.5	100.00	9.89	2.08	1.26	1.26
PC 0.6-3.0*	100.00	19.78	4.16	2.52	2.52
PC 0.6-4.0*	100.00	26.37	5.55	3.36	3.36

*These samples were mixed with 21.1 wt-% NaCl. The rest were mixed with 4.8 wt-% NaCl.

Formulas used in Tables A.3.1 and A.3.2:

$$m_{NaCl} = \%NaCl \cdot w_{NaCl}$$

Where w_{NaCl} is the weighed in NaCl solution, $\%NaCl$ is the concentration of the NaCl solution in wt-% and m_{NaCl} is the mass of NaCl in the sample.

$$m_{Cl} = m_{NaCl} \cdot \frac{M_{Cl}}{M_{NaCl}}$$

Where M_{Cl} is the molar mass of chlorine (35.45 g/mol), M_{NaCl} is the molar mass of natrium chloride (58.44 g/mol) and m_{Cl} is the mass of Cl in the sample.

$$\%Cl_{cem} = \frac{m_{Cl}}{m_{cement}}$$

Where m_{cement} is the mass of cement in the sample and $\%Cl$ is the chloride concentration in the sample in wt-% of cement.

8.4 Appendix A.4 – Raw data from potentiometric titration of cement paste samples

Table A.4.1: Raw data from potentiometric titration of cement paste samples with w/c = 0.4. Volume of filtrate and AgCl are given in millilitres. Mass of cement paste is given in grams. The moisture content, %Moisture, is given in wt-% of cement paste at 105°C.

Sample parallel	V_{AgCl}	$V_{filtrate}$	$m_{cement\ paste}$	%Moisture	$\%Cl_{paste\ 105°C}$	$\%Cl_{dry\ cement}$
PC 0.4-0.0_1	-	5.0	1.0	13.5 %	invalid	invalid
PC 0.4-0.0_2	-	5.0	1.0	13.5 %	invalid	invalid
PC 0.4-0.2_1	0.3089	2.5	1.0	13.0 %	0.252	0.298
PC 0.4-0.2_2	0.3039	2.5	1.0	13.0 %	0.248	0.293
PC 0.4-0.4_1	0.4760	2.5	1.0	14.5 %	0.395	0.459
PC 0.4-0.4_2	0.4749	2.5	1.0	14.5 %	0.394	0.458
PC 0.4-1.5_1	0.5619	1.0	1.0	14.5 %	1.165	1.353
PC 0.4-1.5_2	0.5569	1.0	1.0	14.5 %	1.155	1.341
PC 0.4-3.0_1	0.8497	1.0	1.0	14.0 %	1.751	2.047
PC 0.4-3.0_2	0.9230	1.0	1.0	14.0 %	1.902	2.223
PC 0.4-4.0_1	0.7084	0.5	1.0	14.5 %	2.937	3.413
PC 0.4-4.0_2	0.7130	0.5	1.0	14.5 %	2.956	3.435

Table A.4.2: Raw data from potentiometric titration of dement paste samples with w/c = 0.6. Volume of filtrate and AgCl are given in millilitres. Mass of cement paste is given in grams. The moisture content, %Moisture, is given in wt-% of cement paste at 105°C.

Sample parallel	V_{AgCl}	$V_{filtrate}$	$m_{cement\ paste}$	%Moisture	$\%Cl_{paste\ 105°C}$	$\%Cl_{dry\ cement}$
PC 0.6-0.0_1	0.0503	10.0	1.0	18.5 %	0.011	0.013
PC 0.6-0.0_2	0.0512	10.0	1.0	18.5 %	0.011	0.013
PC 0.6-0.2_1	0.2705	2.5	1.0	18.0 %	0.234	0.272
PC 0.6-0.2_2	0.2843	2.5	1.0	18.0 %	0.246	0.286
PC 0.6-0.4_1	0.4078	2.5	1.0	19.5 %	0.359	0.410
PC 0.6-0.4_2	0.4111	2.5	1.0	19.5 %	0.362	0.414
PC 0.6-1.5_1	0.5177	1.0	1.0	20.0 %	1.147	1.302
PC 0.6-1.5_2	0.5168	1.0	1.0	20.0 %	1.145	1.300
PC 0.6-3.0_1	0.8530	1.0	1.0	19.5 %	1.878	2.146
PC 0.6-3.0_2	0.8432	1.0	1.0	19.5 %	1.857	2.121
PC 0.6-4.0_1	0.5779	0.5	1.0	18.5 %	2.514	2.908
PC 0.6-4.0_2	0.5727	0.5	1.0	18.5 %	2.492	2.882

8.5 Appendix A.5 – Error propagation calculations

All of the relative uncertainties related to the potentiometric titration of the cement paste and mortar samples in the thesis were calculated by error propagation [25]. The uncertainties used in the error propagation calculations are given in Table A.5.

Table A.5: Relative uncertainties of the variables used in the potentiometric titration

Variable	**Relative uncertainty [%]**
Concentration AgCl	0.01
Volume AgCl (equivalence point)	0.01
Volume HNO_3	0.02
Volume filtrate (5 ml pipette)	0.05
Volume filtrate (1 ml pipette)	0.001
Mass of cement paste	0.01
Percentage of water from TGA	0.001

8.6 Appendix A.6 – Chloride content from potentiometric titration of concrete samples

Table A.6.1: Chloride content by weight of concrete at 105 °C of sample 2-B-2.

Layer [mm]	$\%Cl_{conc\ 105\ °C}$
0-5	0.290
5-10	0.407
10-15	0.397
15-20	0.379
20-25	0.369
25-30	0.380
30-40	0.341
40-50	0.282
50-60	0.279
60-70	0.203
70-80	0.235
80-90	0.168
90-100	0.144

Table A.6.2: Chloride content by weight of concrete at 105 °C of sample 2-T-2.

Layer [mm]	$\%Cl_{conc\ 105\ °C}$
0-5	0.254
5-10	0.308
10-15	0.283
15-20	0.193
20-25	0.155
25-30	0.145
30-40	0.114
40-50	0.082

Table A.6.3: Chloride content by weight of concrete at 105 °C of sample RSD.

Layer [mm]	$\%Cl_{conc\ 105\ °C}$
0-5	0.590
5-10	0.614
10-15	0.486
15-20	0.437
20-30	0.454
30-40	0.415
40-50	0.325
50-60	0.314

Table A.6.4: Chloride content by weight of concrete at 105 °C of sample BAR.

Layer [mm]	$\%Cl_{conc\ 105\ °C}$
0-3	0.433
3-6	0.343
6-10	0.285
10-15	0.247
15-20	0.183
20-30	0.079
30-40	0.020
40-50	0.005

8.7 Appendix A.7 – Counts per second and area percentage of aggregates of concrete samples

Table A.7.1: Counts per second of the cement paste phase (CPS) and area percentage of aggregates ($\%Agg_{\mu\text{-}XRF}$) based on S-Ca-Si-elemental map, S-Ca-elemental map and S-elemental map in concrete sample 2-T-2.

	S-Ca-Si-map		**S-Ca-map**		**S-map**	
Layer [mm]	**$\%Agg_{\mu\text{-}XRF}$**	**CPS**	**$\%Agg_{\mu\text{-}XRF}$**	**CPS**	**$\%Agg_{\mu\text{-}XRF}$**	**CPS**
0-5	59.8 %	18.5	66.6 %	20.4	61.2 %	19.1
5-10	61.8 %	18.7	57.1 %	17.5	56.1 %	17.2
10-15	51.9 %	13.2	59.1 %	14.8	58.3 %	14.7
15-20	53.9 %	11.3	52.5 %	11.7	53.4 %	11.8
20-25	56.8 %	9.60	56.7 %	9.55	53.7 %	9.21
25-30	57.3 %	7.28	60.8 %	7.64	59.4 %	7.54
30-40	60.3 %	5.71	61.8 %	5.77	57.3 %	5.47
40-50	49.5 %	3.82	51.8 %	3.90	50.9 %	3.87

Table A.7.2: Counts per second of the cement paste phase (CPS) and area percentage of aggregates ($\%Agg_{\mu\text{-}XRF}$) based on a S-Ca-Si-map in concrete sample 2-B-2.

Layer [mm]	**$\%Agg_{\mu\text{-}XRF}$**	**CPS**
0-5	51.2 %	38.8
5-10	80.6 %	39.0
10-15	63.5 %	27.8
15-20	56.2 %	25.9
20-25	63.8 %	22.3
25-30	65.4 %	21.6
30-40	69.2 %	20.3
40-50	64.9 %	15.1
50-60	62.5 %	13.8
60-70	57.7 %	13.2
70-80	48.8 %	10.2
80-90	64.6 %	9.05
90-100	57.9 %	7.56

Table A.7.3: Counts per second of the cement paste phase (CPS) and area percentage of aggregates ($\%Agg_{\mu\text{-}XRF}$) based on a S-Ca-Si-elemental map in concrete sample BAR.

Layer [mm]	**$\%Agg_{\mu\text{-}XRF}$**	**CPS**
0-3	51.7 %	9.13
3-6	63.9 %	11.2
6-10	47.0 %	11.3
10-15	57.4 %	10.8
15-20	60.2 %	8.91
20-30	57.4 %	5.51
30-40	55.1 %	2.42
40-50	58.8 %	1.96

Table A.7.4: Counts per second of the cement paste phase (CPS) and area percentage of aggregates ($\%Agg_{\mu\text{-}XRF}$) based on a S-Ca-Si-elemental map in concrete sample RSD.

Layer [mm]	**$\%Agg_{\mu\text{-}XRF}$**	**CPS**
0-5	74.2 %	35.8
5-10	66.9 %	36.5
10-15	61.0 %	25.0
15-20	63.5 %	22.5
20-30	61.3 %	16.3
30-40	58.1 %	11.6
40-50	66.1 %	9.74
50-60	62.6 %	8.65

8.8 Appendix A.8 – Values used in the calculation of the chloride content based on different elemental maps

The values in Tables A.8.1 to A.8.3 are the basis for the chloride contents of sample 2-T-2 for different elemental maps (see Figure 25). For all tables $\%Cl_{paste\ \mu\text{-}XRF}$ is the chloride content by weight of cement paste and has been calculated by use of the calibration curve (see Chapter 5.2). $\%Cl_{conc\ \mu\text{-}XRF}$ is the chloride content by weight of concrete and has been calculated with the calculation model (see Chapter 2.5). $\%Cl_{conc\ 105\ °C}$ is the chloride by weight of concrete at 105 °C determined by titration.

Table A.8.1: Values based on a sulphur-elemental map.

Layer [mm]	**$\%Cl_{paste\ \mu\text{-}XRF}$ [wt-% of paste]**	**$\%Cl_{conc\ \mu\text{-}XRF}$ [wt-% of concrete]**	**$\%Cl_{conc\ 105\ °C}$ [wt-% of concrete]**	**$\%Cl_{conc\ \mu\text{-}XRF}$ - $\%Cl_{conc\ 105\ °C}$ [wt-% of concrete]**
0-5	0.92	0.293	0.254	0.04
5-10	0.83	0.302	0.308	-0.01
10-15	0.70	0.240	0.283	-0.04
15-20	0.55	0.215	0.193	0.02
20-25	0.42	0.161	0.155	0.01
25-30	0.33	0.110	0.145	-0.04
30-40	0.22	0.079	0.114	-0.04
40-50	0.14	0.058	0.082	-0.02

Table A.8.2: Values based on a sulphur-calcium-elemental map.

Layer [mm]	**$\%Cl_{paste\ \mu\text{-}XRF}$ [wt-% of paste]**	**$\%Cl_{conc\ \mu\text{-}XRF}$ [wt-% of concrete]**	**$\%Cl_{conc\ 105\ °C}$ [wt-% of concrete]**	**$\%Cl_{conc\ \mu\text{-}XRF}$ - $\%Cl_{conc\ 105\ °C}$ [wt-% of concrete]**
0-5	0.99	0.266	0.254	0.01
5-10	0.84	0.299	0.308	-0.01
10-15	0.70	0.236	0.283	-0.05
15-20	0.54	0.216	0.193	0.02
20-25	0.43	0.155	0.155	0.00
25-30	0.33	0.107	0.145	-0.04
30-40	0.24	0.074	0.114	-0.04
40-50	0.14	0.058	0.082	-0.02

Table A.8.3: Values based on a sulphur-calcium-silica-elemental map.

Layer [mm]	**$\%Cl_{paste\ \mu\text{-}XRF}$ [wt-% of paste]**	**$\%Cl_{conc\ \mu\text{-}XRF}$ [wt-% of concrete]**	**$\%Cl_{conc\ 105\ °C}$ [wt-% of concrete]**	**$\%Cl_{conc\ \mu\text{-}XRF} - \%Cl_{conc\ 105\ °C}$ [wt-% of concrete]**
0-5	1.04	0.342	0.254	0.09
5-10	1.05	0.327	0.308	0.02
10-15	0.72	0.291	0.283	0.01
15-20	0.61	0.234	0.193	0.04
20-25	0.51	0.181	0.155	0.03
25-30	0.37	0.130	0.145	-0.01
30-40	0.27	0.089	0.114	-0.03
40-50	0.16	0.069	0.082	-0.01

8.9 Appendix A.9 – Values used in the calculation of the chloride content in concrete by µ-XRF and application of the calculation model

The values in Tables A.9.1 to A.9.4 are the basis for the plots in Figure 27 in Chapter 5.5. For all tables $\%Cl_{paste\ \mu\text{-}XRF}$ is the chloride content by weight of cement paste and has been calculated by use of the calibration curve (see Chapter 5.2). $\%Cl_{conc\ \mu\text{-}XRF}$ is the chloride content by weight of concrete and has been calculated with the calculation model (see Chapter 2.5). $\%Cl_{conc\ 105\ °C}$ is the chloride by weight of concrete at 105 °C determined by titration.

Table A.9.1: $\%Cl_{paste\ \mu\text{-}XRF}$, $\%Cl_{conc\ \mu\text{-}XRF}$, $\%Cl_{conc\ 105\ °C}$ and the difference between $\%Cl_{conc\ \mu\text{-}XRF}$ and $\%Cl_{conc\ 105\ °C}$ for sample 2-T-2.

Layer [mm]	**$\%Cl_{paste\ \mu\text{-}XRF}$ [wt-% of paste]**	**$\%Cl_{conc\ \mu\text{-}XRF}$ [wt-% of concrete]**	**$\%Cl_{conc\ 105\ °C}$ [wt-% of concrete]**	**$\%Cl_{conc\ \mu\text{-}XRF}$ - $\%Cl_{conc\ 105\ °C}$ [wt-% of concrete]**
0-5	1.04	0.342	0.254	0.09
5-10	1.05	0.327	0.308	0.02
10-15	0.72	0.291	0.283	0.01
15-20	0.61	0.234	0.193	0.04
20-25	0.51	0.181	0.155	0.03
25-30	0.37	0.130	0.145	-0.01
30-40	0.27	0.089	0.114	-0.03
40-50	0.16	0.069	0.082	-0.01

Table A.9.2: $\%Cl_{paste\ \mu\text{-}XRF}$, $\%Cl_{conc\ \mu\text{-}XRF}$, $\%Cl_{conc\ 105\ °C}$ and the difference between $\%Cl_{conc\ \mu\text{-}XRF}$ and $\%Cl_{conc\ 105\ °C}$ for sample 2-B-2.

Layer [mm]	**$\%Cl_{paste\ \mu\text{-}XRF}$ [wt-% of paste]**	**$\%Cl_{conc\ \mu\text{-}XRF}$ [wt-% of concrete]**	**$\%Cl_{conc\ 105\ °C}$ [wt-% of concrete]**	**$\%Cl_{conc\ \mu\text{-}XRF}$ - $\%Cl_{conc\ 105\ °C}$ [wt-% of concrete]**
0-5	2.25	0.924	0.290	0.63
5-10	2.26	0.339	0.407	-0.07
10-15	1.60	0.473	0.397	0.08
15-20	1.48	0.539	0.379	0.16
20-25	1.26	0.371	0.369	0.00
25-30	1.22	0.341	0.380	-0.04
30-40	1.14	0.281	0.341	-0.06
40-50	0.83	0.237	0.282	-0.05
50-60	0.75	0.230	0.279	-0.05
60-70	0.72	0.253	0.203	0.05
70-80	0.54	0.237	0.235	0.00
80-90	0.47	0.136	0.168	-0.03
90-100	0.38	0.134	0.144	-0.01

Table A.9.3: $\%Cl_{paste\ \mu\text{-}XRF}$, $\%Cl_{conc\ \mu\text{-}XRF}$, $\%Cl_{conc\ 105\ °C}$ and the difference between $\%Cl_{conc\ \mu\text{-}XRF}$ and $\%Cl_{conc\ 105\ °C}$ for sample BAR.

Layer [mm]	**$\%Cl_{paste\ \mu\text{-}XRF}$ [wt-% of paste]**	**$\%Cl_{conc\ \mu\text{-}XRF}$ [wt-% of concrete]**	**$\%Cl_{conc\ 105\ °C}$ [wt-% of concrete]**	**$\%Cl_{conc\ \mu\text{-}XRF}$ - $\%Cl_{conc\ 105\ °C}$ [wt-% of concrete]**
0-5	2.21	0.60	0.590	0.01
5-10	1.62	0.51	0.614	-0.10
10-15	1.45	0.36	0.486	-0.12
15-20	1.12	0.31	0.437	-0.12
20-30	0.78	0.24	0.454	-0.21
30-40	0.57	0.18	0.415	-0.23
40-50	0.46	0.10	0.325	-0.22
50-60	0.43	0.14	0.314	-0.18

Table A.9.4: $\%Cl_{paste\ \mu\text{-}XRF}$, $\%Cl_{conc\ \mu\text{-}XRF}$, $\%Cl_{conc\ 105\ °C}$ and the difference between $\%Cl_{conc\ \mu\text{-}XRF}$ and $\%Cl_{conc\ 105\ °C}$ for sample BAR.

Layer [mm]	**$\%Cl_{paste\ \mu\text{-}XRF}$ [wt-% of paste]**	**$\%Cl_{conc\ \mu\text{-}XRF}$ [wt-% of concrete]**	**$\%Cl_{conc\ 105\ °C}$ [wt-% of concrete]**	**$\%Cl_{conc\ \mu\text{-}XRF}$ - $\%Cl_{conc\ 105\ °C}$ [wt-% of concrete]**
0-3	0.48	0.19	0.433	-0.24
3-6	0.60	0.18	0.343	-0.17
6-10	0.61	0.27	0.285	-0.01
10-15	0.58	0.20	0.247	-0.05
15-20	0.46	0.15	0.183	-0.03
20-30	0.26	0.09	0.079	0.01
30-40	0.08	0.03	0.020	0.01
40-50	0.05	0.02	0.005	0.01

8.10 Appendix A.10 – Details of the sensitivity analysis

The sensitivity analysis was performed by increasing or decreasing the slope of the calibration curve and the area percentage of aggregates in each layer. The calculation model was then applied on the changed slope or area percentage of aggregates. Only one of the variables were changed at a time. The output from the calculation model is the chloride content by weight of concrete. This content was then subtracted from the chloride content by weight of concrete determined by potentiometric titration. If the difference obtained was negative, it was changed to an absolute value. The absolute values of the differences of the layers beyond 10 mm was then averaged. By changing only one variable at a time, one can determine the impact of said variable. The slope and the area percentage of aggregates were increased by 15% and decreased by 15%. The increase and decrease of the slope were calculated by multiplying the original slope by 1.15 and 0.85, respectively. The same method was applied when increasing and decreasing the percentage of aggregates in each layer. By doing so, one has four average absolute differences that can be compared to the original average absolute difference of the established technique. As an example, the values for the sensitivity analysis of sample BAR and a 15% increase of the slope are shown below.

w/c-ratio	0.4	
Density of aggregates	2700	kg/m^3
Density of cement	3150	kg/m^3
Density of paste	1951	kg/m^3

Slope	16.47
Y-intercept	1.13

Percentage change of slope	15 %

Percentage change of area percentage of aggregates	0 %

Layer [mm]	%Cl from titration [wt-% of concrete]	CPS	Area percentage of aggregates [%]	%Cl in cement paste [wt-% of cement paste]	%Cl in concrete [wt-% of concrete]	Difference [wt-% of concrete]	Absolute difference [wt-% of concrete]
0-3	0.433	9.13	51.70 %	0.42	0.17	0.26	0.26
3-6	0.343	11.24	63.90 %	0.53	0.15	0.19	0.19
6-10	0.285	11.26	47.00 %	0.53	0.24	0.04	0.04
10-15	0.247	10.77	57.40 %	0.51	0.18	0.07	0.07
15-20	0.183	8.91	60.20 %	0.41	0.13	0.05	0.05
20-30	0.079	5.51	57.40 %	0.23	0.08	0.00	0.00
30-40	0.02	2.42	55.10 %	0.07	0.03	-0.01	0.01
40-50	0.005	1.96	58.80 %	0.04	0.01	-0.01	0.01
						Average from 10-50 mm	0.03

9 References

1. Bertolini, L., et al., *Corrosion of Steel in Concrete : Prevention, Diagnosis, Repair*. 2013, Weinheim, GERMANY: John Wiley & Sons, Incorporated.
2. Hansson, C.M. and B. Sorensen, *Threshold concentration of chloride in concrete for the initiation of reinforcement corrosion.* ASTM Special Technical Publication, 1990(1065): p. 3-16.
3. Angst, U., et al., *Critical chloride content in reinforced concrete - A review.* Cement and Concrete Research, 2009. **39**(12): p. 1122-1138.
4. RILEM, *Draft recommendation for repair strategies for concrete structures damaged by reinforcement corrosion.* Materials and Structures, 1994. **27**(7): p. 415-436.
5. Fluge, F., *Marine chlorides. A probabilistic approach to derive provisions for EN206-1.* 3rd DuraNet Workshop, Tromso, Norway, 10-12-July., 2001, 2001.
6. De Weerdt, K., H. Justnes, and M.R. Geiker, *Changes in the phase assemblage of concrete exposed to sea water.* Cement and Concrete Composites, 2014. **47**(Supplement C): p. 53-63.
7. Danner, T., K. De Weerdt, and M. Geiker, *μ-XRF characterisation of chloride ingress and self-healing in cracked concrete*. 2017.
8. Alzyoud, S., H.S. Wong, and N.R. Buenfeld, *Influence of reinforcement spacers on mass transport properties and durability of concrete structures.* Cement and Concrete Research, 2016. **87**: p. 31-44.
9. Bruker Nano GmbH, *M4 Tornado User Manual*, Bruker, Editor. 2015: Berlin.
10. Standard Norge. *NS-EN 197-1 Composition, specifications and conformity criteria for common cements*. 2011 [cited 2017 Oct]; Available from: https://www.standard.no/no/abonnement/standarder.
11. De Weerdt, K., et al., *Towards the understanding of chloride profiles in marine exposed concrete, impact of leaching and moisture content.* Construction and Building Materials, 2016. **120**: p. 418-431.
12. Standard Norge. *NS-EN 196-2 Methods of testing cement Part 2: Chemical analysis of cement*. 2005 [cited 2018 April]; Available from: https://www.standard.no/no/abonnement/standarder.
13. Standard Norge. *NS-EN 206 Concrete - Specification, performance, production and conformity*. 2014 [cited 2017 Oct]; Available from: https://www.standard.no/no/abonnement/standarder.
14. Standard Norge. *NS-EN 196-1 Methods of testing cement Part 1: Determination of Strength*. 2005 [cited 2018 April]; Available from: https://www.standard.no/no/abonnement/standarder.
15. Tokyay, M., *Cement and concrete mineral admixtures*. 2016, CRC Press, Taylor & Francis Group. p. 96.
16. Escadeillas, G. and J.C. Maso, *Approach of the initial state in cement paste, mortar, and concrete.* Advances in Cementitious Materials, 1991. **16**: p. 169-184.
17. Bård Espelid et al., *Reinforcement corrosion in marine concrete structures under dynamic loading.* 1987.
18. Standard Norge. *NS 427 A Betongarbeider*. 1962.
19. Kompen, R., *Betongregelverk relatert til bestandighet - Betongbruer i et historisk perspektiv*, in *Fagdag 2014 for Statens Vegvesen*. 2014.
20. J.P. Holtmon and H.R. Iskasen, *Utvikling av kloridbestandig betong - Rapport fra produksjon av prøveelementer*. 1994, Vegdirektoratet: Oslo, Norway.

21. Jacobsen, S., ed. *Concrete Technology*. 2016, Norwegian University of Science and Technology: Trondheim.
22. Shi, Z., et al., *Friedel's salt profiles from thermogravimetric analysis and thermodynamic modelling of Portland cement-based mortars exposed to sodium chloride solution.* Cement and Concrete Composites, 2017. **78**: p. 73-83.
23. Wahid, F.A., *Characterising concrete using micro X-ray fluorescence (μXRF)*. 2016, Imperial College London.
24. Mettler Toledo. *Sodium Chloride - Concentration vs. density (20°C)*. [cited 2018 April]; Available from: https://www.mt.com/no/no/home/supportive_content/concentration-tables-ana/Sodium_Chloride_de_e.html.
25. Hardvard University. *Summary Rules for Error Propagation*. [cited 2018; Available from: https://sites.fas.harvard.edu/~scphys/nsta/error_propagation.pdf.